

NASA CONTRACTOR  
REPORT

NASA CR-144294

SPACE PROCESSING FLOAT ZONE THERMAL ANALYSIS

By J. T. Pogson and D. M. Anderson

The Boeing Company  
Seattle, Washington

May 1976

(NASA-CF-144294) SPACE PROCESSING FLCAT  
ZONE THERMAL ANALYSIS (Boeing Co., Seattle,  
Wash.) 62 p HC \$4.50

N76-25059

CSCI 20B

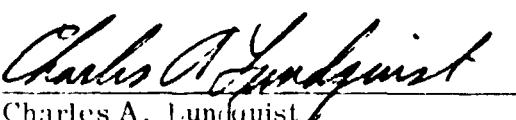
Unclass

G3/76 28245

Prepared for

NASA-GEORGE C. MARSHALL SPACE FLIGHT CENTER  
Marshall Space Flight Center, Alabama 35812

RECEIVED  
NASA STI FACILITY  
INPUT BRANCH

TECHNICAL REPORT STANDARD TITLE PAGE			
1. REPORT NO. <b>NASA CR-144294</b>	2. GOVERNMENT ACCESSION NO.	3. CLIENT CATALOG NO.	
4. TITLE AND SUBTITLE <b>Space Processing Float Zone Thermal Analysis</b>		5. REPORT DATE <b>May 1976</b>	
6. PERFORMING ORGANIZATION CODE			
7. AUTHOR(S) <b>J. T. Pogson and D. M. Anderson</b>	8. PERFORMING ORGANIZATION REPORT NO.		
9. PERFORMING ORGANIZATION NAME AND ADDRESS <b>The Boeing Company Seattle, Washington</b>	10. WORK UNIT NO.		
11. CONTRACT OR GRANT NO. <b>NAS8-31635</b>		13. TYPE OF REPORT & PERIOD COVERED	
12. SPONSORING AGENCY NAME AND ADDRESS <b>National Aeronautics and Space Administration Washington, D. C. 20546</b>		Contractor	
14. SPONSORING AGENCY CODE			
15. SUPPLEMENTARY NOTES Prepared under the technical monitorship of James M. Zwiener, Space Sciences Laboratory, Marshall Space Flight Center, Alabama 35812			
16. ABSTRACT <p>Two thermal analysis (BETA) computer program adaptations were prepared to analyze phase change histories in crystal specimens: the first program (BETA-CYL) treats right circular cylinder configurations and the second, more general, program (BETA-BOR) treats a generalized body-of-revolution configuration. A series of computer runs were made for silicon material to determine boundary conditions which produce flat solidification interfaces while, at the same time, minimizing peak temperatures in the molten zone. Flat solidification interfaces are a goal believed by some investigators to be required to produce high quality semiconductor materials. The thermal effects of convection in a molten zone were examined and found to be negligible in comparison to the conduction heat transfer of the melt.</p>			
17. KEY WORDS		18. DISTRIBUTION STATEMENT Unclassified—Unlimited	
		 Charles A. Lundquist Director, Space Sciences Laboratory	
19. SECURITY CLASSIF. (of this report) <b>Unclassified</b>	20. SECURITY CLASSIF. (of this page) <b>Unclassified</b>	21. NUMBER OF PAGES <b>58</b>	22. EFFIC. <b>NTIS</b>

## TABLE OF CONTENTS

	PAGE
LIST OF FIGURES	iv
LIST OF TABLES	v
1.0 INTRODUCTION	1
2.0 ANALYSIS	2
3.0 DISCUSSION OF RESULTS	4
3.1 Cylindrical Melt Zones	5
3.2 Body of Revolution Melt Zones	9
CONCLUSIONS	11

ORIGINAL PAGE IS  
OF POOR QUALITY

## LIST OF FIGURES

	PAGE
<b>FIGURE 1</b> MATH MODEL	15
2 BETA PROGRAM - CRYSTAL MELT/FREEZE TRANSIENT STUDY	16
3 HEAT PULSE SUBROUTINE (QSFC)	17
4 RUN 49 & 55 - LOCAL SURFACE HEAT FLUX PROFILES	18
5 PHASE CHANGE SUBROUTINE (PHAS)	19
6 RUN 71 - TEMPERATURE GRADIENT & HEAT FLUX PROFILES	20
7 RUN 71 - MELT ZONES	21
8 RUN 75 STEADY-STATE - NO CONVECTION	23
9 RUN 82 STEADY STATE - INFINITE CONVECTION	24
10 RUN 29 MELT ZONES	25
11 RUN 36 MELT ZONES	27
12 RUN 39 MELT ZONES	29
13 RUN 40 MELT ZONES	30
14 RUN 44 MELT ZONES	32
15 RUN 49 MELT ZONES	34
16 RUN 55 MELT ZONES	37
17 RUN 56 MELT ZONES	38
18 RUN 60 MELT ZONES	41
19 RUN 62 MELT ZONES	43
20 RUN 65 MELT ZONES	45
21 SURFACE HEAT FLUX RUN 56 & 60	47
22 SURFACE HEAT FLUX RUN 62	48
23 RUN 60 - TEMPERATURE GRADIENT & HEAT FLUX PROFILES	49
24 RUN 62 - TEMPERATURE GRADIENT & HEAT FLUX PROFILES	50
25 RUN 65 - TEMPERATURE GRADIENT & HEAT FLUX PROFILES	51
26 TYPICAL BODY OF REVOLUTION CONFIGURATIONS	52
27 BODY OF REVOLUTION NODE MAP	53
28 RUN 80 - MELT ZONE - TIME = 0	54
29 RUN 80 - MELT ZONE - TIME = 2.852 MIN.	55
30 RUN 72 - MELT ZONE NODE MAP	56
31 MELT ZONE TIME = 0 RUN 72	57
32 MELT ZONE TIME = 7.3 MIN. RUN 72	58

## LIST OF TABLES

	Page
TABLE 1    COMPUTER RUN SUMMARY	12
2           SILICON THERMAL CONDUCTIVITY	13
3           SILICON SPECIFIC HEAT	14

## 1.0 INTRODUCTION

Growth of single crystals in vertical arc-imaging furnaces has been successfully demonstrated by various researchers. Early experiments with these furnaces using a carbon-arc energy source, encountered difficulties in maintaining uniform light intensity for required periods of time. Development of high-power Xenon arc lamps substantially reduced the instability problem experienced with carbon-arcs, and also allowed longer-term operation for crystal growth. Experiments have shown that one of the preferred approaches for growing single crystals in arc-imaging furnaces is the pedestal technique. This technique has alternatively been labeled a modified Czochralski, or modified float-zone process. The principal advantage of the float-zone process over other crystal growth techniques is production of higher purity crystals; achieved by eliminating the need for a crucible and the resulting crucible contamination. The homogeneity of crystals grown by the float-zone process, as with other processes, is affected by circulation patterns in the molten semi-conductor material. Carruthers and Grasso have extensively studied the stability and fluid flow in floating zones in both a simulated zero-gravity environment and on Skylab. Effects of convection patterns on homogeneity of solute distribution and electrical resistivity have been reviewed by Benson. Similar considerations should apply to float-zone crystal growth, and indicate that for the Czochralski process, all convection in the melt should be avoided.

Growth of single crystals in space is expected to substantially improve the solute homogeneity of crystals, by reducing or eliminating convection within the melt region. It should also be possible to form larger diameter crystals because the length of the suspended liquid zone can be increased in the absence of gravity.

Maintaining a large-diameter uniform-temperature melt zone will be a key problem in designing a crystal growth experiment using a solar concentrator. Accordingly, this study has been directed at thermal modeling of the liquid zone to predict temperature gradients for various parametric changes.

## 2.0 ANALYSIS

Two generalized lumped parameter nodal math models were formulated to represent a right circular cylindrical, BETA-CYL, and a body of revolution configuration, BETA-BOR, with time varying boundary conditions. The physical system was sectioned into an array of discrete volumes and the mass of each volume element was "lumped" at a point within the volume which it represented. The paths for heat transfer from one mode to another were represented by conductors joining the appropriate nodes. The thermal models each contained a maximum of 300 nodes, Figure (1) depicts the right circular cylindrical nodal math model.

The thermal math models described above were input into the Boeing Engineering Thermal Analyzer Program (BETA). This program solves an electrical analog network system using an iterative numerical method. Both transient and steady state solutions are treated. A logic diagram of the computer program detailing the computational steps is given in Figure (2). Several BETA subroutines required development to permit numerical simulation of the applied heat flux boundary conditions and the change of phase process.

The heat pulse subroutine is illustrated in Figure (3). This permits the specification of an externally applied heat flux of the form:

$$q_i = q_0 e^{-A|X-Vt - B|^2}$$

where:

- $q_0$  - Peak surface heat flux, Btu/min-in<sup>2</sup>
- X - Distance from reference end of crystal, inches
- V - Pulse velocity away from reference end of crystal, in/min
- t - Time elapsed since start of pulse movement, min
- B - Starting position of center of pulse measured from reference end of crystal, inches
- A - Pulse width parameter

Values of A of 100 and 4 were used, the relative widths of the heat pulses can be seen in Figure 4.

A similar cooling subroutine was also formulated to represent surface cooling.

During a phase change each node must receive or release a quantity of energy equal to its latent heat of fusion. This energy exchange accounting system was simulated by a phase change subroutine, PHAS. Figure (5) illustrates the logic system. Each node is surveyed to see if it is at or undergoing a phase change. If it is undergoing a phase change then an accounting system keeps the nodal temperature constant at the melting temperature until the energy exchange matches the node latent heat of fusion.

This study did not directly consider the transparency of silicon to thermal radiation; however, the "no convection" and "Infinite convection" extremes considered for energy transport in the molten zone could be expected to bound the effects which might be observed had internal radiation been considered. Furthermore, with a cylindrical crystal, any radiation interchange between the surroundings and crystal internal regions due to transparency can only tend to reduce radial temperature gradients and consequently give a more uniform axial flow of thermal energy which is required to obtain flat interfaces. Radiation interchange in the axial direction, between internal crystal regions, was not expected to be very significant as temperature differences within the crystal are much less than temperature differences which exist between the crystal and its surroundings.

### 3.0 DISCUSSION OF RESULTS

A total of 82 runs were made to de-bug, checkout, and perform production analyses for this study. Only the runs shown in Table 1 contained significant results. The other runs, although more numerous, were less significant in terms of expended machine time.

The first block on this table describes the crystal configuration for each run and refers to a right circular cylinder unless otherwise stated. The right circular cylinder crystals were considered to consist of 30 wafers of equal thickness as defined by planes normal to the cylinder axis (see "Wafer Thickness" column).

The surface heat flux refers to the peak surface heat flux of a Gaussian shaped pulse when the word "Gauss" appears in the "Pulse Width" column. If the word "Uniform" appears in the "Pulse Width" column, the surface heat flux value applies over the entire heated length, and the number appearing in the "Pulse Width" column is the heated length, in inches, of a section of cylinder centered along the cylinder axis.

For some runs, the peak surface heat flux,  $q_0$ , was reduced linearly with time; the  $q_0$  limits where applicable, are described in the "Surface Heat Flux" column. In any case, when the run time, i.e. "Real Time" in the "Time Data" block, exceeds the time shown in the "Heat Time" column, the heat is reduced to zero after the "Heat Time" shown.

In the "Number of Nodes" column, "300" indicates that each wafer was considered to consist of 10 rings, the temperatures of which were computed as node temperatures by the program. The number "120" indicates each wafer was considered to consist of 4 rings.

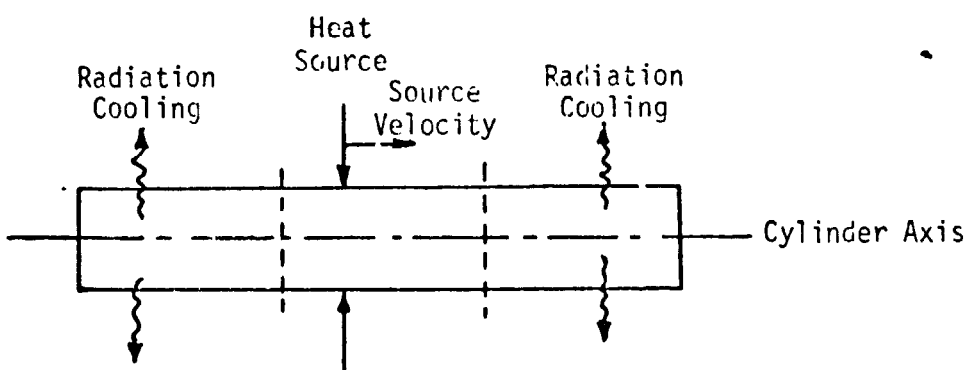
Under the "Cooling Parameters" block, the "Sink Temperature" and "Script F" define radiation rates from the radial surface of the crystal for the axial length of surface specified in the "Cooled Area" column. The ends; normal to the cylinder axis, were considered insulated for all runs.

Except for Runs 35, 72, 75, 80, 81, and 82, the initial temperature, uniform throughout the crystal, was one degree Fahrenheit below the melting point. This was done to prevent wasted computer time raising the crystal to the melting point. Runs 72, 75, 80, 81, and 82 were intended to determine steady state conditions and estimates of the final temperatures were used as initial temperatures for the analysis to conserve machine time, i.e., initial temperatures above the melting point were used in the heated region, and temperatures somewhat below the melting point were used in the cooled region.

Run 35 was a check of the program against an analytical solution for a cylinder, with uniform constant surface heat flux, using an initial uniform temperature of zero; excellent agreement was obtained.

### 3.1 Cylindrical Melt Zones

The initial part of this study consisted of analyzing cylindrical specimens (BETA-CYL program) on a transient basis using a constant strength heat source moving in the axial direction with ends cooled by radiation to a 70°F environment as shown below:



The source of the incident radiant energy was not modeled since it was considered that it could be best treated after determining the boundary conditions required to produce flat interfaces. The following parameters were varied in the transient analyses: heated length, cooled length, specimen diameter, constant source strength (moving heat sources), and transient source strength (moving and fixed heat sources). It was determined that an adiabatic section

between the heated and cooled sections would be beneficial in producing flat interfaces. Additionally, it was found that excessive machine time was required with a transient-type analysis due to the rather low solidification rate required for growth of high-perfection crystals ( $\approx 1$  cm/hr). A preferable analytical technique, in comparison to the transient analysis, for treating the continuous zone refinement/growth along a rod was to obtain the steady-state solutions for configurations with stationary boundary conditions which give flat interfaces. If an extremely slow feed rate of the specimen is then introduced after steady state is achieved, a negligible change in the shape and location of the interfaces would occur with respect to a fixed reference system. Machine time required to solve for steady-state conditions is nominal provided that reasonable estimates of the final conditions are provided as inputs.

Figure 6 describes the conditions and results for Run 71. Excellent flat-interface solidification conditions were obtained and are shown in Figure 7. The physical state of each ring of each wafer has been represented in the computer printout by an "0", "1", or "2". Each column of figures represents a wafer of the crystal as defined in Table 1. The radial width of each wafer, as defined in the program, varies so that the volumes of each ring are equal regardless of the nominal ring radii. The figures are, therefore, not to scale in the radial direction. Since all wafers are the same thickness in the axial direction (for the right circular cylinder configuration) the printouts are to scale in the axial direction. The axis of the cylinder is indicated by a centerline at each end of the crystal. A "0" indicates that the state of that node is solid. A "1" indicates a molten state, and "2" indicates a partially melted state at the melting temperature. A column of zeros adjacent to a column of twos or ones indicates a flat solidification interface within a one-wafer-thickness tolerance. These printouts were used as a visual tool to allow rapid scanning of run results for each case. More exact definition of interface shapes can be determined by inspection of node freezing fraction data in the computer result numerical output.

The data printed at the left of each state are:

Time - minutes from start of analysis  
 $G_{A\text{MAX}}$  - maximum axial temperature gradient, °F/inch  
 $G_{R\text{MAX}}$  - maximum radial temperature gradient, °F/inch  
 $T_{\text{MAX}}$  - maximum temperature, °F

A melting point temperature of 2573°F was assumed for silicon. Conductivity and specific heat values employed as a function of temperatures are shown in supplementary Tables 2 and 3.

Run 71 was for a 1-inch diameter crystal, 7.5 inches long with a stationary uniformly irradiating heat source applied to the central 2 inches of specimen. The source strength decayed linearly from 20 Btu/min-in<sup>2</sup> to 0 in the first 2 minutes of run time. For approximately 7 minutes after the heat source was shut off, the central molten zone solidified with virtually flat interfaces. The solidification rate was approximately 40 cm/hr, which is higher than current state of the art. The solidification process, however, could be increased to any desired duration by reducing the cooling rate at the crystal ends, e.g., through the use of louvers or radiation shields. The simulated high solidification rate was used here to conserve machine time. A lower cooling rate would be accompanied by lower temperature gradients in the crystal compared to those shown on Figures 6 and 7.

Figures 8 and 9 contain the computation for runs 75 and 82 respectively. A section through one half of the length of crystal is shown with each node defined by a rectangle (to scale), with resulting steady state temperatures given at each node in degrees F. The melt interface shape was sketched in based on freezing fraction data from the numerical output of the program.

A nearly converged solution using the steady state analysis technique was obtained with the case analyzed in Run 75; the corresponding conditions and results are shown on Figure 8. Although there was a slight deviation from flatness at the interface, it is believed that this could be eliminated by a slight reduction in the rate of

source irradiation which would move the interface into the insulated (shielded) region where the thermal flux lines are more nearly straight.

To bound the effects of convection in the molten zone, an "infinite convection" analysis was performed for the same configuration as in Run 75. This condition was implemented by assigning a cup-mixing temperature to the melt at each iteration which has the effect of instantaneously distributing throughout the melt zone all incident energy at the surface. The results are shown in Run 82, Figure 9. A virtually flat interface was obtained in almost the same position as with no convection. By comparing figures 8 and 9 it is seen that there is little difference in the two solutions except that the melt temperature with convection is uniform at a value somewhat lower than the peak value observed with no convection. The degree of convergency to a steady state solution can be assessed by noting how closely the total cooling rate approaches the constant heating rate. For Runs 75 and 82 the errors are 3% and 1% respectively, which is sufficient convergence for preliminary purposes.

Additional transient results, Runs 29, 36, 39, 40, 44, 49, 55, 56, 60, 62 and 65, similar to those presented for Run 71 are shown in Figures 10 through 20. The significant results for each of these runs are shown in the "Comments" column of Table 1.

Crystal specimen dimensions and boundary conditions are shown on Figures 4, 21, and 22 for Runs 49, 55, 56, 60, and 62. Of particular interest are the heat pulse shapes and positions on the specimen as a function of time which cannot be readily visualized from Table 1 data.

For Runs 60, 62, and 65 maximum axial and radial temperature gradients, maximum temperature, and peak surface heat flux are shown as a function of time on Figures 23, 24, and 25 respectively. The irregularities in the temperature and gradient curves are due to (1) the results of a lumped parameter thermal analysis, e.g. at the instant when a node melts or solidifies, a relatively sudden adjustment in adjacent node temperatures occurs, and (2) the location of the peak temperature and gradients moves around

in the crystal, whereas, the plots show only the peak values regardless of location in the crystal.

### 3.2 Body of Revolution Melt Zones

The body-of-revolution program (BETA-BOR) has the capability to analyze configurations where the specimen has a shape more complex than a right circular cylinder. Possible configurations of interest are shown on Figure 26: (a) vertical cylinder float zone with gravity (b) float-zone in Zero-G with rotation, and (c) crystal growth from different sized feed stock. An example of case (c) was analyzed for 6-inch and 12-inch rods meeting in a molten zone with an assumed curved section transition; the configuration and boundary conditions are shown on Figure 27. Estimates of steady state conditions used for program input are shown in Figure 28. Conditions after 2.35 minutes are shown on Figure 29. Steady state convergence is approached with a good flat solidification interface on the 12-inch end. The interface shapes were sketched in on Figure 29, based on melt fraction data from the program output for the respective interface nodes.

Figure 27 shows the locations of the nodes for Run 80 as limited by the ability of the node size to be resolved into cells on the printout page. The dashes and asterisks are used in an alternate fashion for each wafer to define the node boundaries for each wafer. Each wafer has 10 ring shaped nodes, however on the 6" diameter end, not all are shown due to the resolution limitation described above. The radial interfaces between the nodes in regions of body diameter change are considered by the program to be conical surfaces. The uniform irradiation rate shown for the heated area is based on actual surface area, not a correct area based on some assumed ray direction. The shape shown on the printout is approximately to scale.

Figure 28 shows the initial conditions for Run 20: an asterisk indicates a temperature above the melting point, a dash indicates a temperature below the melting point. The difference between this figure as compared to Figure 7 is that the symbols at each node correspond to the node state rather than alternating to define node boundaries. Final conditions are shown for Run 80 on Figure 29

after the indicated elapsed time, given the Figure 28 initial conditions. Dashes and asterisks are as described for Figure 28 and an "X" symbol denotes a node partially melted at the melting temperature. Melt interface shapes shown are based on freezing fraction data for the melting nodes. Temperatures at selected points were shown for reference. Heating and cooling rates were shown as a guide to the deviation from steady state, i.e. if a true steady state had been reached, heating and cooling rates would be equal. This condition could be achieved by allowing the run to proceed in time, at a corresponding cost in machine time. Figures 30, 31, and 32 show data similar to that of Figures 27, 28, and 29 which apply to Run 72; neither steady state conditions nor flat interfaces were obtained.

## CONCLUSIONS

Thermal math models of a silicon float zone crystal growth process were formulated. Transient temperatures and melt zones were determined for a variety of simulated external heat flux conditions. It was found that nearly flat interface solidification conditions could be simulated by varying the applied heat flux, as in cases 65 and 71. Additionally, convective affects were found to be negligible in reducing temperature gradients.

ORIGINAL PAGE  
OF POOR QUALITY

Table 1. Computer Run Summary

Cylinder configuration		Heating parameters			Nodes			Cooling parameters			Time data			Comments	
Run	Diameter (in)	Length (in)	Water thickness (in)	Heat peak flux (Btu/in <sup>2</sup> min)	Pulse velocity (in/min)	Start pulse width (min)	Number of nodes	Sink temp (°F)	Script file	Elapsed time (min)	Real time (min)	Mach time (sec)			
29	3	3	0.1	10,000	0.1	0.01	100	0.3	ap	—	—	—	05.1	Initial run, stability check with extremely high heat flux.	
30	3	3	0.1	10,000	0.1	0.01	100	0.3	ap	—	—	—	05.1	Pulse surface temp 56,750°F above melting point at end of run	
35	3	3	0.1	10,000	0.1	0.01	300	—	—	—	—	—	9.0	Same as run 1, except pulsed infinite convection and different phase map symbols; convection increases quantity of melting	
75	3	3	0.1	Uniform surface heat flux = 106 Btu/min/in <sup>2</sup>			300	—	—	—	—	—	1.0	Check case for comparison with classical solution - cylinder with uniform surface heat flux - went thru PHAS subroutine with near zero heat of fusion to check sublimation. Excellent agreement with Carstensen's solution	
36	3	9	0.3	600	0.3	0.01	4	gauss	300	70	0.3	3"	0.0	Inadequate cooling - crystal melts out to ends - no convection.	
40	3	9	0.3	100	1	1	3	gauss	300	70	0.3	3"	0.0	Pulse surface temp = 4,630°F above melting point	
41	0.7	6	0.2	200	1.4	1.0	2.3	gauss	300	70	0.5	2"	0.3	Inadequate heating - crystal didn't melt to center - no convection	
44	1.5	6	0.2	228	1.4	1.0	2.3	gauss	100	120	120	0.8	3.0	Executive machine time did not run to end of heating cycle.	
49	1.5	6	0.2	198.0 ± 0.0 linear to 0@ t=3	.48	3.0	2.3	gauss	100	120	120	0.8	3.0	Nearly uniform melt at end of minute 1.52°C. Real surface temp above melting point. First interface at upstream end at t = 2.5 min, first interface at downstream end at t = 2.73 min. Flatness 0.05% at 2.20 min. This may be slight deviation from 1.52°C due to numerical error.	
55	1.5	6	0.2	7.9 ± 0.0 linear to 0@ t=3	0.0 ± 0.3	3.0	3.0	gauss	4	120	120	0.8	2"	0.3	Flat upstream interface @ t = 1.63 min, last boundary @ 2.6. Flat at 1.63 min and 4.04 flatness loc. on right end at 4.56. Good to 5.35 mm, 10% interface solid at end. Nearly flat condition - 0.4" of good crystal. Peak temp = 211°F above melt
56	1.5	6	0.2	0.0 ± 0.0 linear to 0@ t=3	0.0 ± 0.3	3.0	3.0	gauss	4	120	120	0.8	2"	0.3	Summational boundary conditions, stationary drawing heat pulse. Flat interface, sum t = 3.47 to 1.537. 0.8" of good crystal in 1.6 minutes. Peak temp = 60.7°F above melt
50	1.5	6	0.2	22.6 ± 0.0 linear to 0@ t=3	0.0 ± 0.4	4.0	3.0	gauss	120	70	0.8	2"	0.3	Not quite enough heat, max surf temp = 25°C above melt.	
62	1.0	7.5	0.25	linear to 0@ t=2	0.0 ± 0.2	2.0	3.75	gauss	120	70	.5	2.5"	5	Not quite enough heat, max surf temp = 25°C above melt.	
65	1.0	7.5	0.25	30.0 ± 0.0 linear to 0@ t=2	0.0 ± 2	2.0	3.75	uniform	120	70	.5	2.5"	5	About 2" of good crystal but 1.2" left to solidify at 5 min trans	
71	1.0	7.5	0.25	18.0 ± 0.0 linear to 0@ t=2	0.0 ± 2	2.0	—	uniform	120	70	.5	2.0"	10	65.3	2" good crystal @ 40 cm/hr solidification rate
75	1.0	7.5	0.25	3.5	0	—	—	uniform	120	70	.5	2.0"	5	Final temps guaranteed to start, near flat initial interface and steady state obtained. Could infer infinite good crystal by testing w/ old cylinder at very low rate (0.1 cm/min)	
81	1.0	7.5	0.25	3.5	0	—	—	uniform	120	70	.5	2.0"	5	Final temps guaranteed to start, same as run 75 except subroutines called every 64 iterations. Didn't save much time and significantly different results occurred.	
82	1.0	7.5	0.25	3.5	0	—	—	uniform	120	70	.5	2.0"	5	Same conditions as run 75 except infinite convection added. New steady state achieved with flatter interface, but nearly the same as without convection except in melt region temperatures are uniform	
72	BOR 6" to 12" dia 7.5 inches long	1	7.5 Btu/min/in <sup>2</sup> uniform over central 2.5" length	300	70	5	2.75"	trans	7.8	43.3	Poor convergence to steady state. Interfaces not flat				
80	BOR 6" to 12" dia 7.5 inches long	4.2 Btu/min/in <sup>2</sup> uniform over central 2.5" length	300	70	5	2.75"	trans	25	40.4	Poor convergence to steady state. Good interface					

Initial condition is melting point minus one degree except runs 35, 51, 62, 72, and 80

▷ See Table 1 discussion in text for pulse width definition

## SILICON THERMAL CONDUCTIVITY

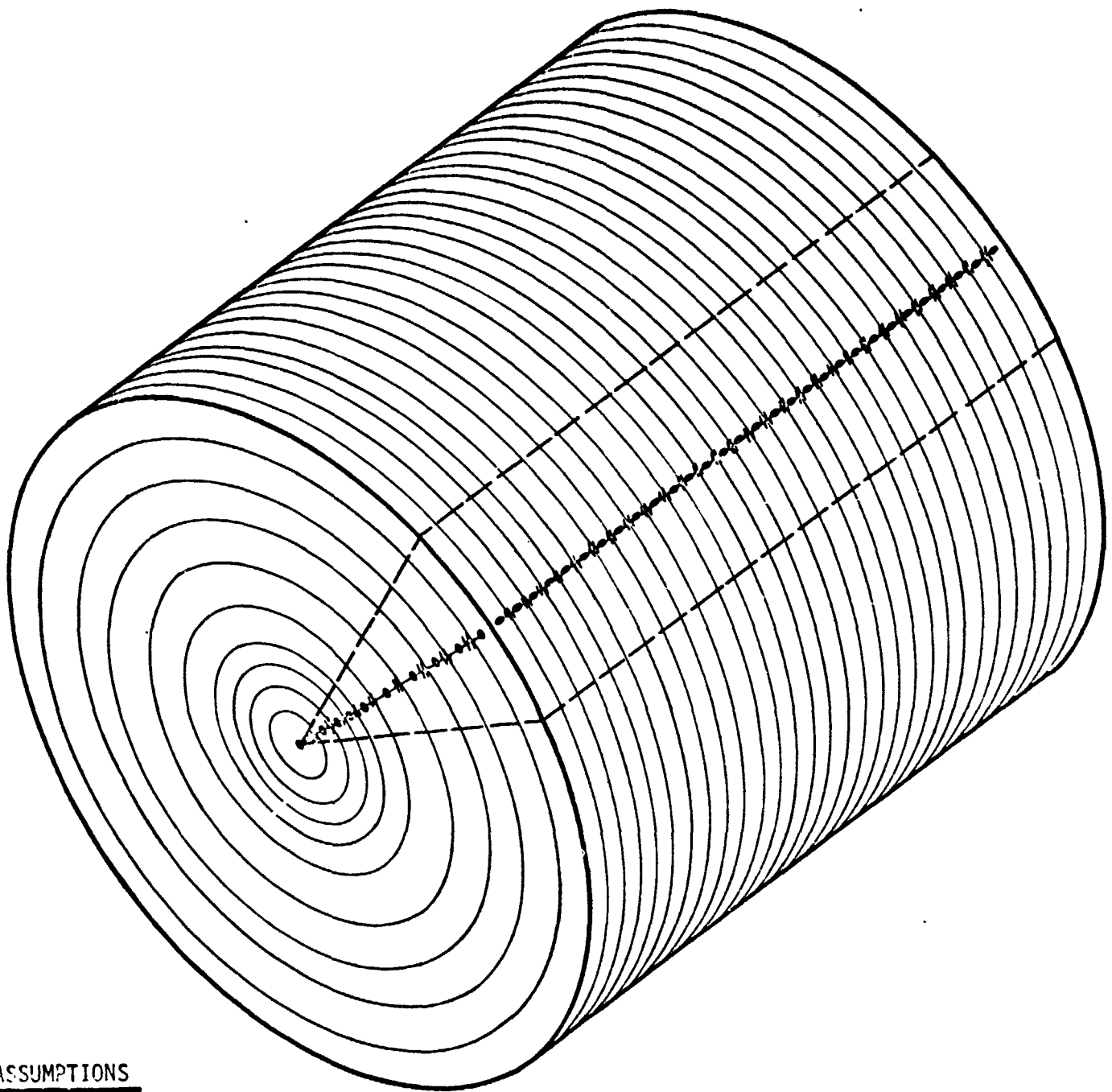
TABLE 2

<u>TEMP -</u>	<u>Thermal Conductivity Btu/min-in-°F</u>
32	.1348
80.3	.1187
170.3	.0955
260.3	.0793
440.3	.0611
620.3	.0497
800.3	.0408
980.3	.0339
1160	.0287
1340	.0250
1520	.0223
1880	.0196
2440	.0178
2573	.0176
$10^6$	.0176

## SILICON SPECIFIC HEAT

TABLE 3

<u>TEMP - °F</u>	<u>Specific Heat - Btu/LB-°F</u>
0	.157
200	.184
400	.197
600	.203
800	.208
1000	.211
1200	.216
1400	.220
1600	.224
1800	.228
2000	.234
2200	.242
2400	.245
2573	.249
2600	.250
$10^6$	.250



#### ASSUMPTIONS

- CENTER CORE + 9 RINGS FOR EACH WAFER - 30 WAFERS
- MASS OF EACH RING OF EACH WAFER IS LUMPED TO FORM NODE (300 NODES)
- ENDS ARE INSULATED
- MOVING GAUSSIAN SURFACE HEAT FLUX DISTRIBUTION
- SURFACE COOLING TO SURROUNDINGS BY RADIATION

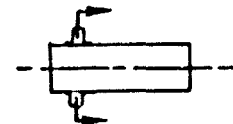
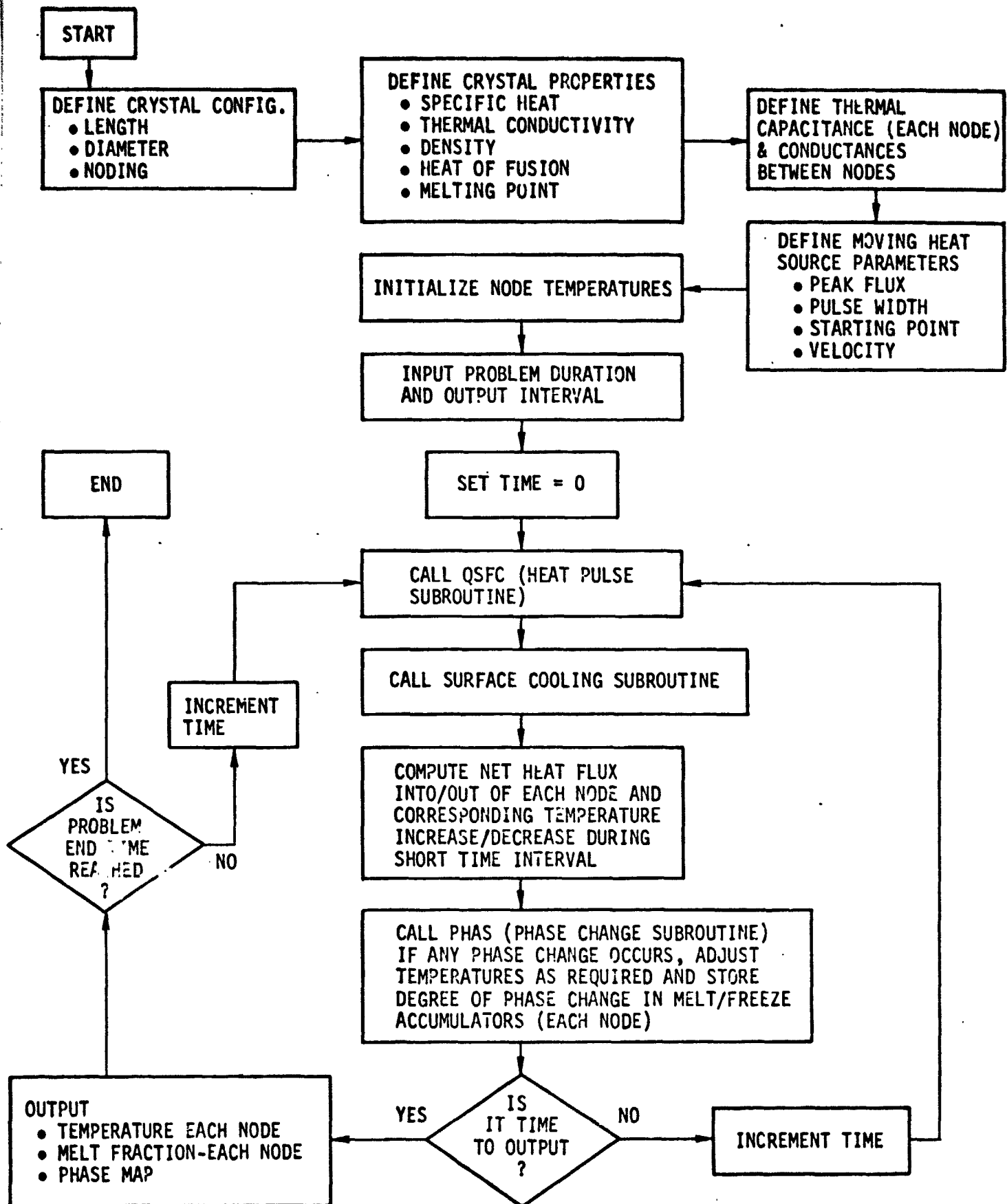


FIGURE: 1 MATH MODEL

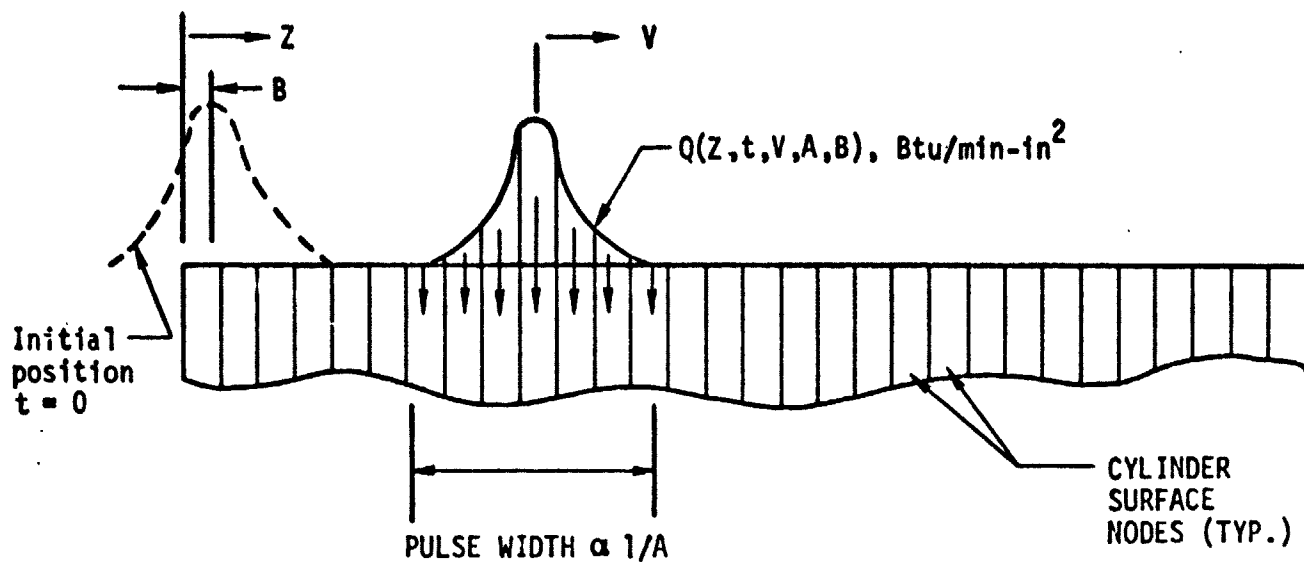
BETA PROGRAM - CRYSTAL MELT/FREEZE TRANSIENT STUDY



ORIGINAL PAGE IS  
OF POOR QUALITY

FIGURE: 2

### HEAT PULSE SUBROUTINE (QSFC)



### FLOW DIAGRAM

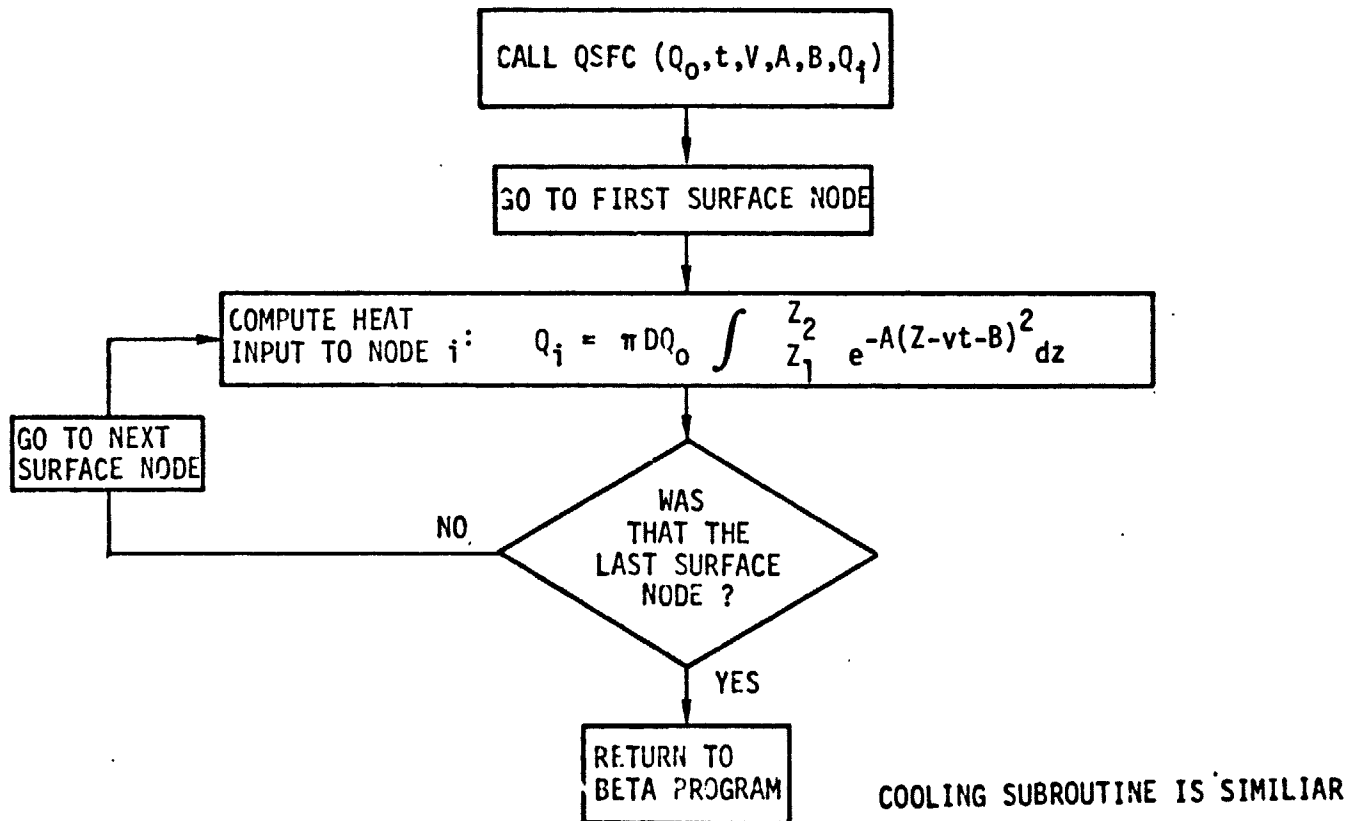
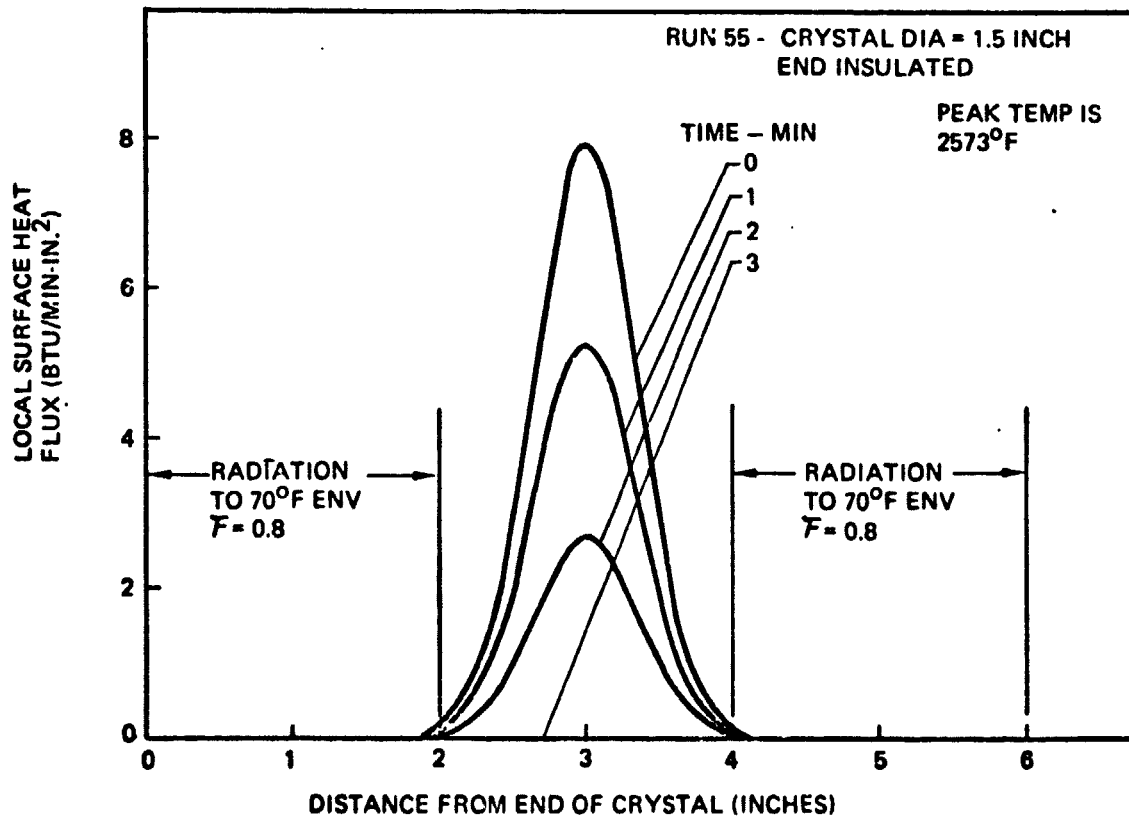
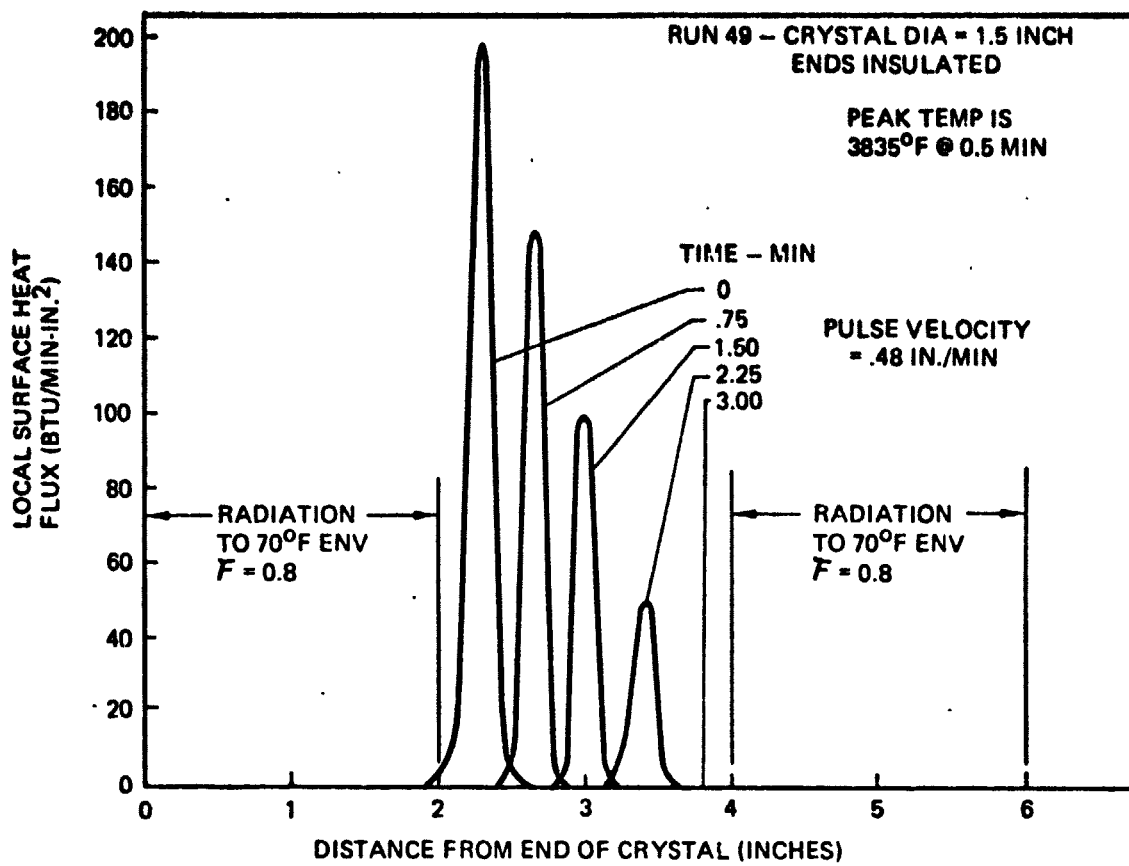


FIGURE: 3



*Figure 4*  
RUN 49 & 55 - LOCAL SURFACE HEAT FLUX PROFILES

## PHASE CHANGE SUBROUTINE (PHAS)

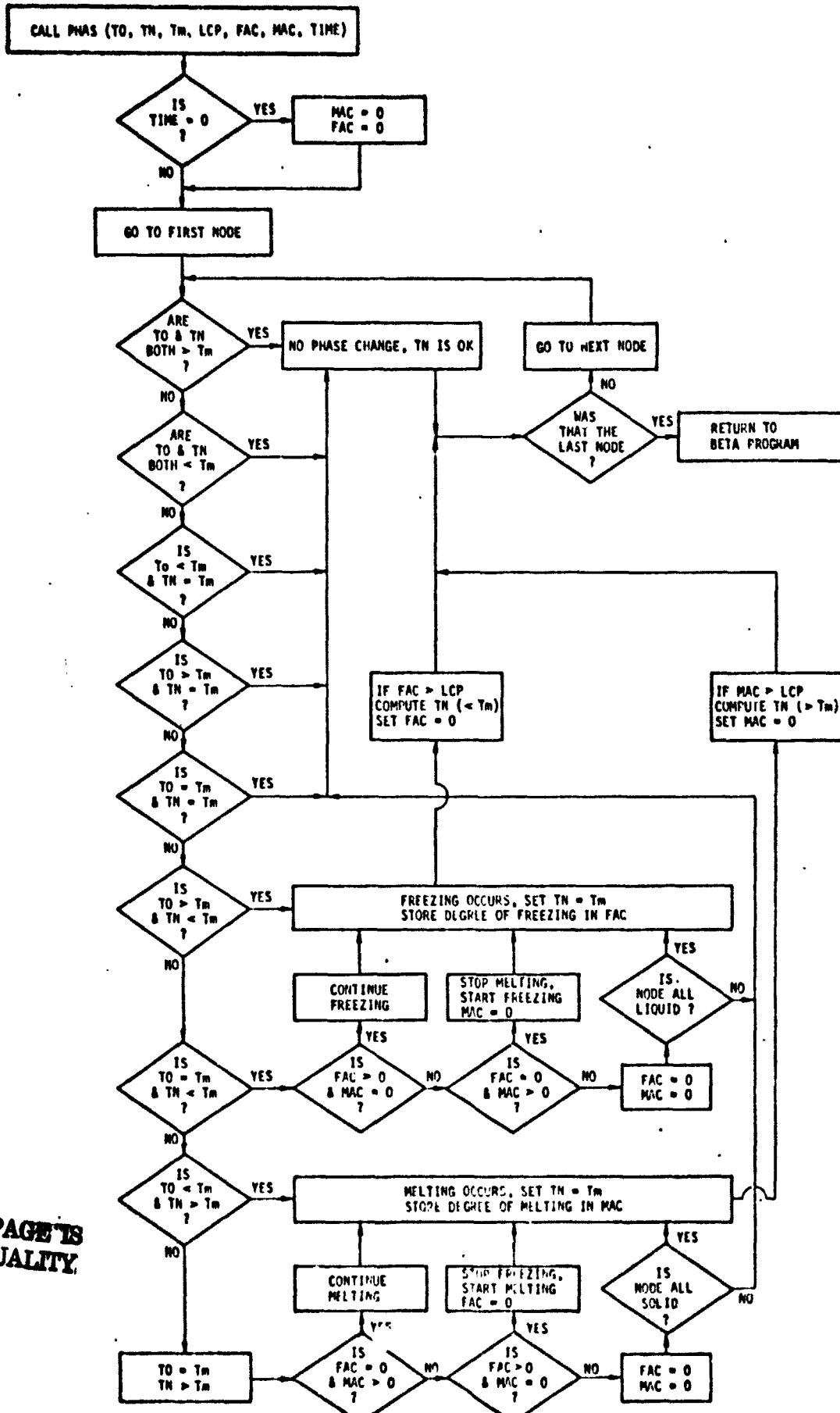


FIGURE : 5

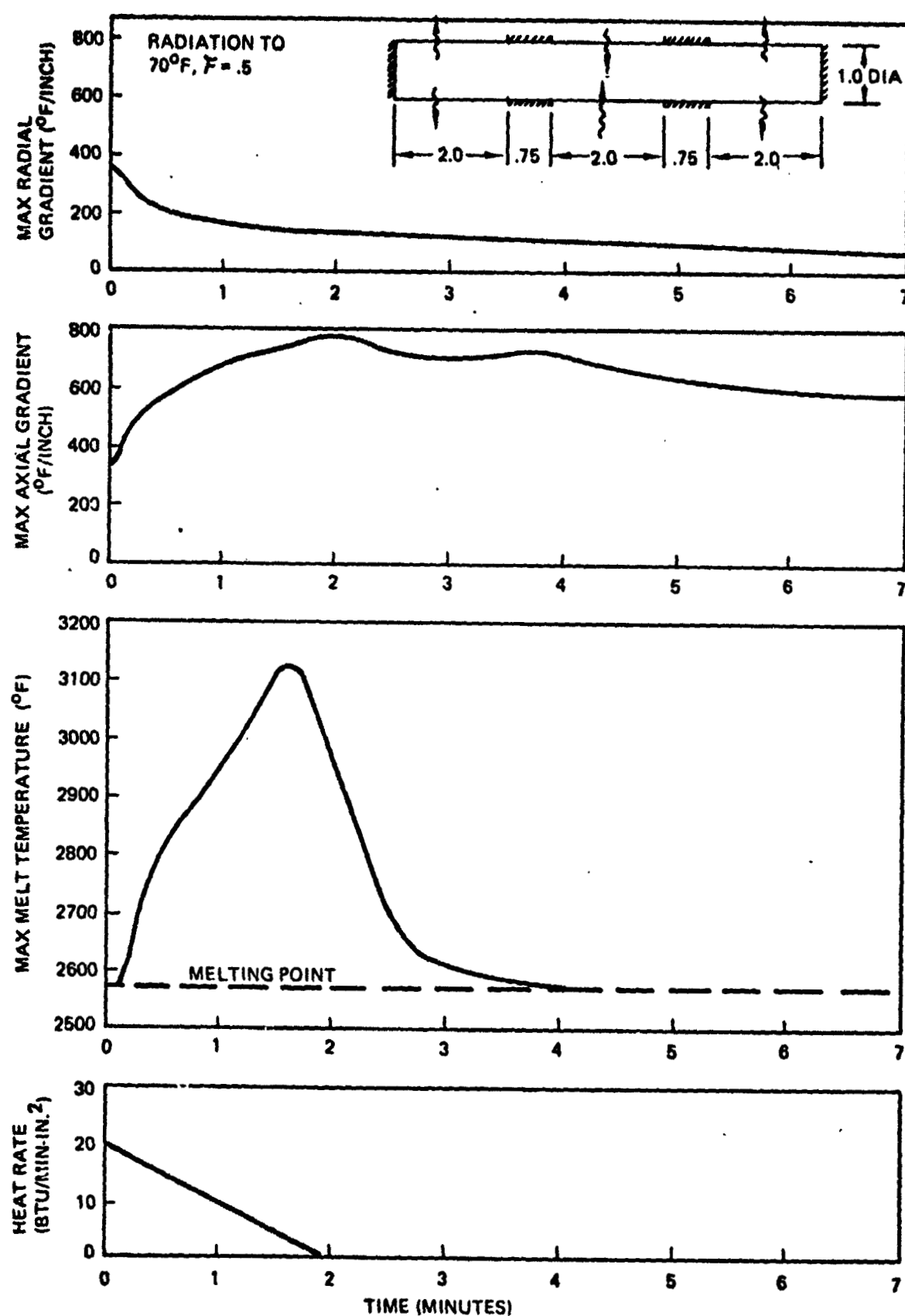


FIGURE 6  
RUN 71 - TEMPERATURE GRADIENT & HEAT FLUX PROFILES

ORIGINAL PAGE IS  
OF POOR QUALITY

TIME= 0.04375

$G_A_{max} = 310$   
 $G_R_{max} = 342$   
 $T_{max} = 2573.$

TIME= 0.39437

$G_A_{max} = 668$   
 $G_R_{max} = 166$   
 $T_{max} = 2956.$

TIME= 0.43750

$G_A_{max} = 464$   
 $G_R_{max} = 280$   
 $T_{max} = 2623.$

TIME= 0.19687

$G_A_{max} = 707$   
 $G_R_{max} = 158$   
 $T_{max} = 2921.$

TIME= 0.70500

$G_A_{max} = 553$   
 $G_R_{max} = 220$   
 $T_{max} = 2749.$

TIME= 1.13750

$G_A_{max} = 728$   
 $G_R_{max} = 147$   
 $T_{max} = 3117.$

TIME= 1.50594

$G_A_{max} = 741$   
 $G_R_{max} = 142$   
 $T_{max} = 3135.$

TIME= 1.42187

$G_A_{max} = 789$   
 $G_R_{max} = 138$   
 $T_{max} = 3052.$

TIME= 0.83125

$G_A_{max} = 639$   
 $G_R_{max} = 175$   
 $T_{max} = 2951.$

TIME= 1.31031

$G_A_{max} = 668$   
 $G_R_{max} = 166$   
 $T_{max} = 2956.$

Figure 7. Run 71 - MELT ZONES

TIME= 2.33750  
 $G_A_{max} = 734$   
 $G_R_{max} = 129$   
 $T_{max} = 2782.$   
 -----

TIME= 2.96719  
 $G_A_{max} = 714$   
 $G_R_{max} = 116$   
 $T_{max} = 2612.$   
 -----

TIME= 3.88125  
 $G_A_{max} = 727$   
 $G_R_{max} = 119$   
 $T_{max} = 2576.$   
 -----

TIME= 4.10469  
 $G_A_{max} = 680$   
 $G_R_{max} = 107$   
 $T_{max} = 2574.$   
 -----

TIME= 5.01094  
 $G_A_{max} = 604$   
 $G_R_{max} = 90$   
 $T_{max} = 2573.$   
 -----

TIME= 7.19219  
 $G_A_{max} = 576$   
 $G_R_{max} = 80$   
 $T_{max} = 2573.$   
 -----

TIME= 8.07612  
 $G_A_{max} = 543$   
 $G_R_{max} = -$   
 $T_{max} = 2573.$   
 -----

TIME= 9.46562  
 $G_A_{max} = 642$   
 $G_R_{max} = 92$   
 $T_{max} = 2573.009$   
 -----

Figure 7 Run 71 (Continued)

ORIGINAL PAGE IS  
OF POOR QUALITY

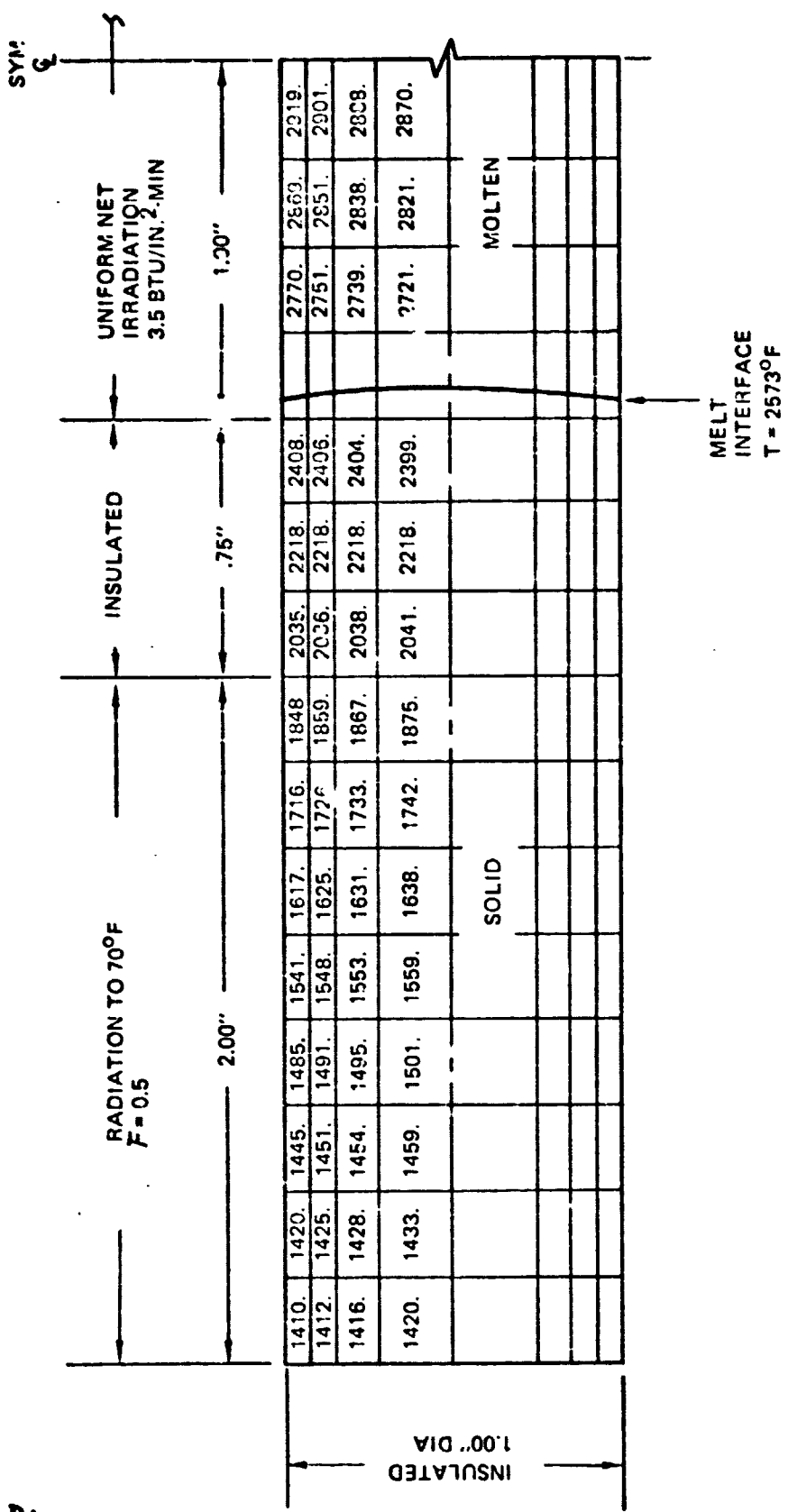
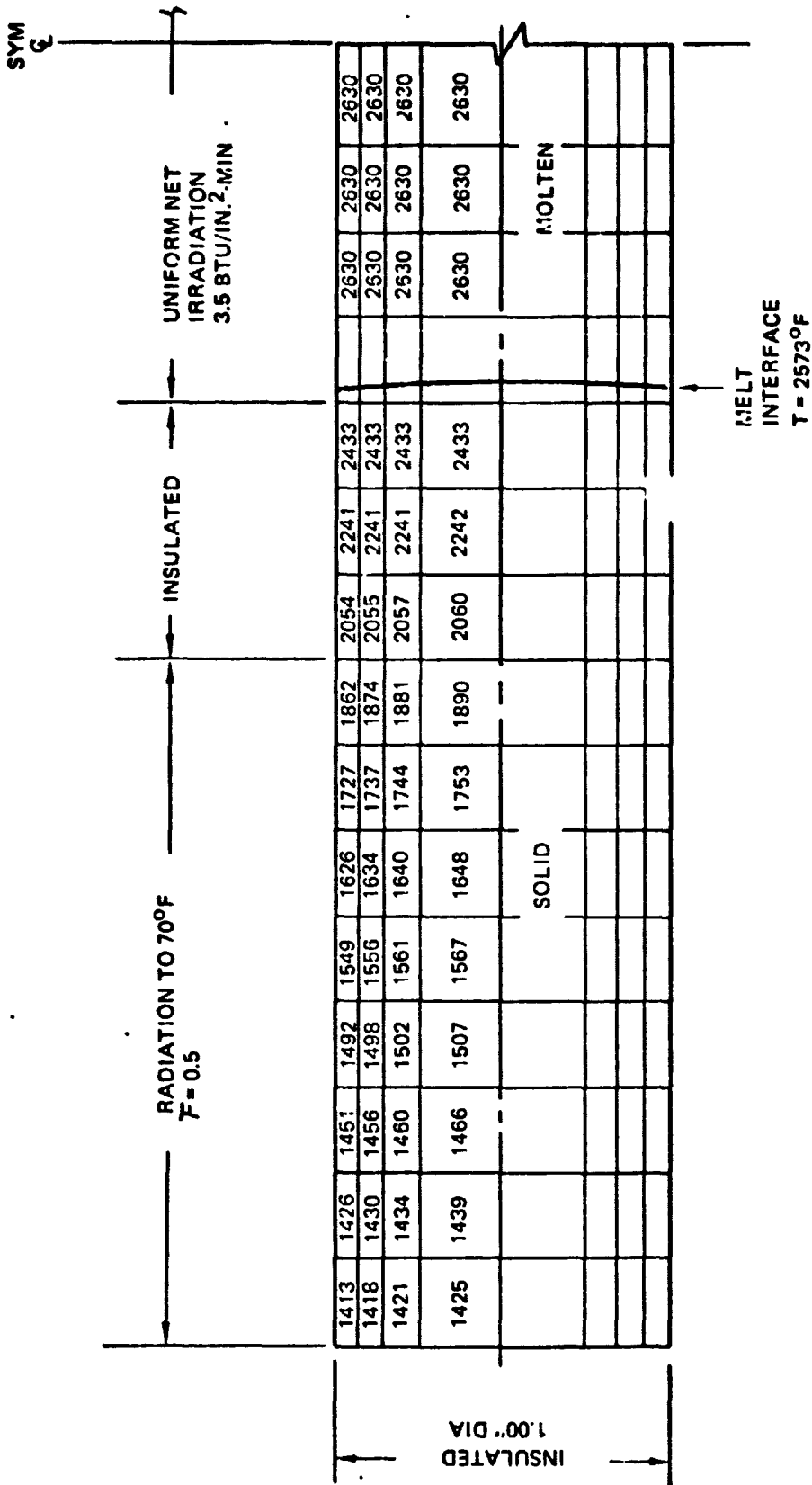


Figure 8. Run 75 STEADY STATE-NO CONVECTION



**Figure 9.** Run 82 STEADY STATE-INFINITE CONVECTION

TIME = 0.03125

ORIGINAL PAGE IS  
OF POOR QUALITY

**FIGURE: 10 . Run 29 - MELT ZONES**

---#HF = ---0.03501-

-THF- C.05000

**Figure 10.** Run 29 (Continued)

TIME = 0.10426

Config 211111120000000000  
Config 021111120000000000  
Config 011111120000000000  
Config 001111120000000000  
Config 000111120000000000  
Config 000011120000000000  
Config 000001120000000000  
Config 000000120000000000  
Config 000000012000000000  
Config 000000001200000000  
Config 000000000120000000  
Config 000000000012000000  
Config 000000000001200000  
Config 000000000000120000  
Config 000000000000012000  
Config 000000000000001200  
Config 000000000000000120  
Config 000000000000000012  
Config 000000000000000001  
Config 000000000000000000

**T MAX = 9.774°F**

TIME = 0.46875

Config 211111120000000000  
Config 021111120000000000  
Config 011111120000000000  
Config 001111120000000000  
Config 000111120000000000  
Config 000011120000000000  
Config 000001120000000000  
Config 000000120000000000  
Config 000000012000000000  
Config 000000001200000000  
Config 000000000120000000  
Config 000000000012000000  
Config 000000000001200000  
Config 000000000000120000  
Config 000000000000012000  
Config 000000000000001200  
Config 000000000000000120  
Config 000000000000000012  
Config 000000000000000001  
Config 000000000000000000

**T MAX = 16.324°F**

TIME = 0.62500

Config 211111120000000000  
Config 021111120000000000  
Config 011111120000000000  
Config 001111120000000000  
Config 000111120000000000  
Config 000011120000000000  
Config 000001120000000000  
Config 000000120000000000  
Config 000000012000000000  
Config 000000001200000000  
Config 000000000120000000  
Config 000000000012000000  
Config 000000000001200000  
Config 000000000000120000  
Config 000000000000012000  
Config 000000000000001200  
Config 000000000000000120  
Config 000000000000000012  
Config 000000000000000001  
Config 000000000000000000

**T MAX = 14.145°F**

TIME = 0.77917

Config 211111120000000000  
Config 021111120000000000  
Config 011111120000000000  
Config 001111120000000000  
Config 000111120000000000  
Config 000011120000000000  
Config 000001120000000000  
Config 000000120000000000  
Config 000000012000000000  
Config 000000001200000000  
Config 000000000120000000  
Config 000000000012000000  
Config 000000000001200000  
Config 000000000000120000  
Config 000000000000012000  
Config 000000000000001200  
Config 000000000000000120  
Config 000000000000000012  
Config 000000000000000001  
Config 000000000000000000

**T MAX = 20.359°F**

ORIGINAL PAGE IS  
OF POOR QUALITY

FIGURE 11 . Run 36 . - MELT ZONES

TIME 1-19376

卷之三

N	TMAX (Solid Circles)	TMAX (Open Circles)
10	0.02	0.01
20	0.04	0.02
30	0.06	0.03
40	0.08	0.04
50	0.10	0.05
60	0.12	0.06
70	0.14	0.07
80	0.16	0.08
90	0.18	0.09
100	0.20	0.10

TIME = 1.045312

TIME = 3.65475

**T<sub>MAX</sub> = 43.676°F**

## FIGURE 11. BUD 36 (Continued)

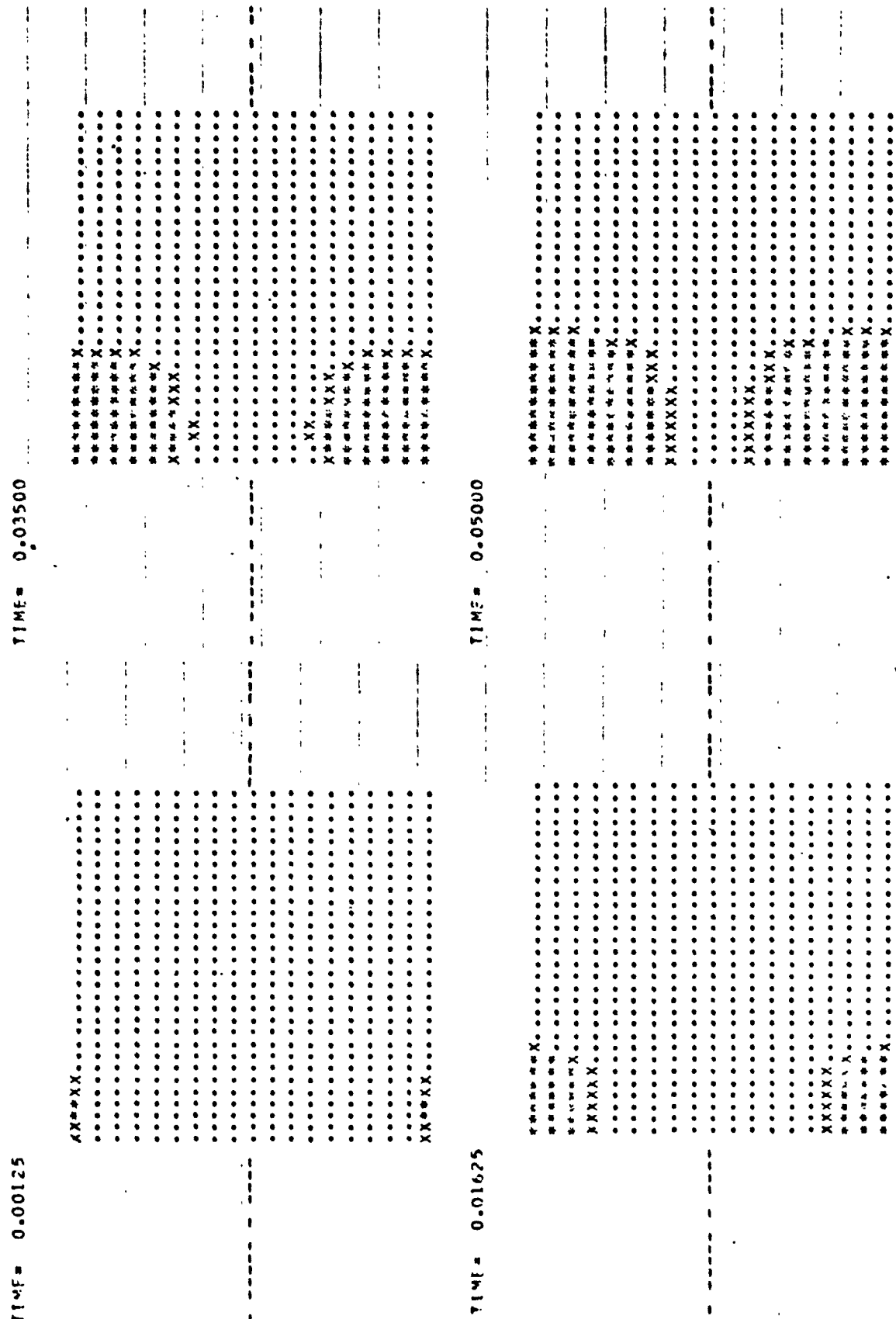


FIGURE: 12 Run 39 - MELT ZONES

ORIGINAL PAGE IS  
OF POOR QUALITY

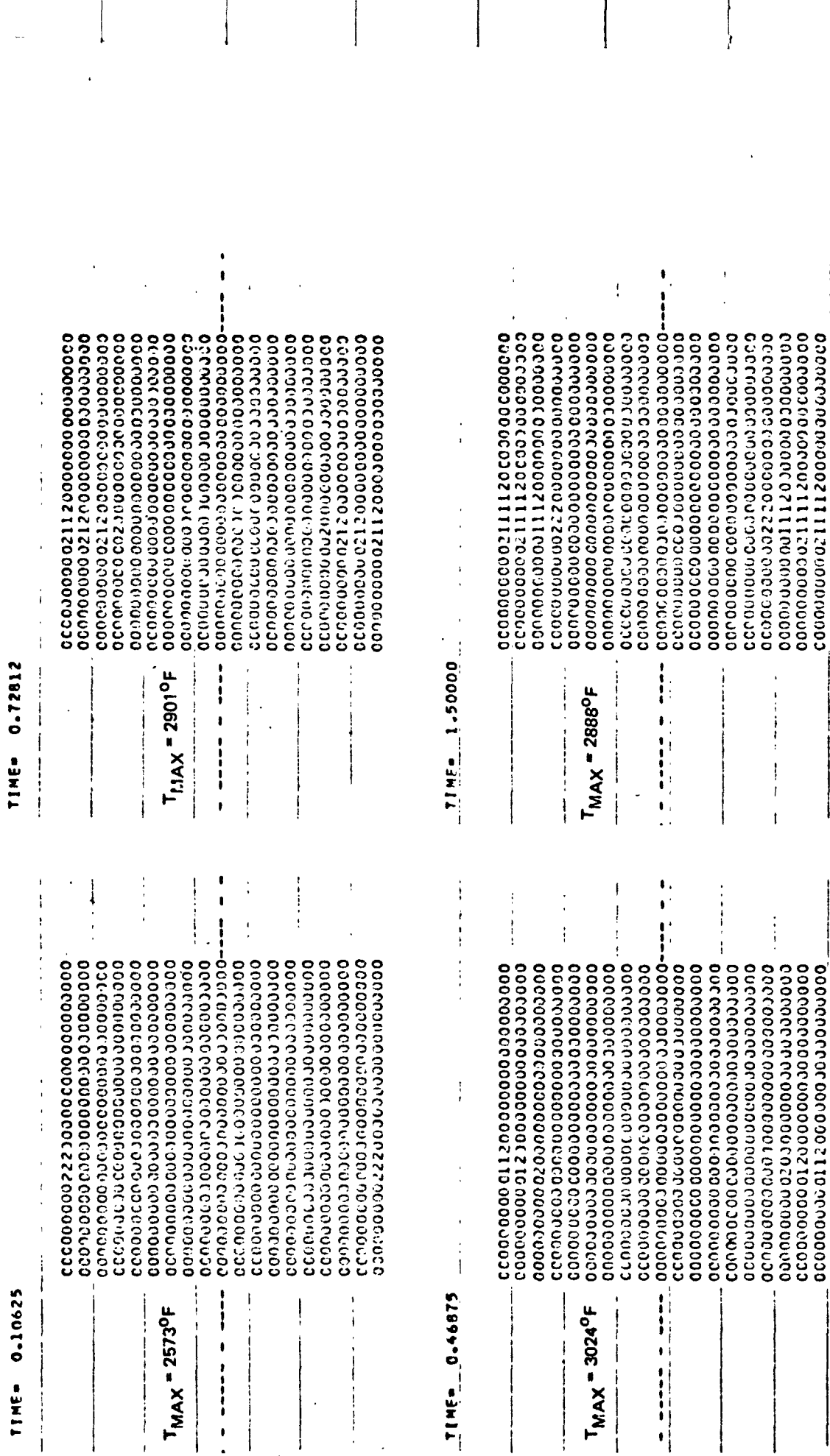


FIGURE: 13 Run 40 - MELT ZONES

TIME = 2:16250

ORIGINAL PAGE IS  
OF POOR QUALITY

TIME 3.17656

T = 387 A 0

$$T_{\text{max}} = 2574^{\circ}\text{F}$$

Volume 2, 61862

TIME 2.43129

אנו

Tsunami = 25730E

**FIGURE 13 : Run 40 (Continued)**

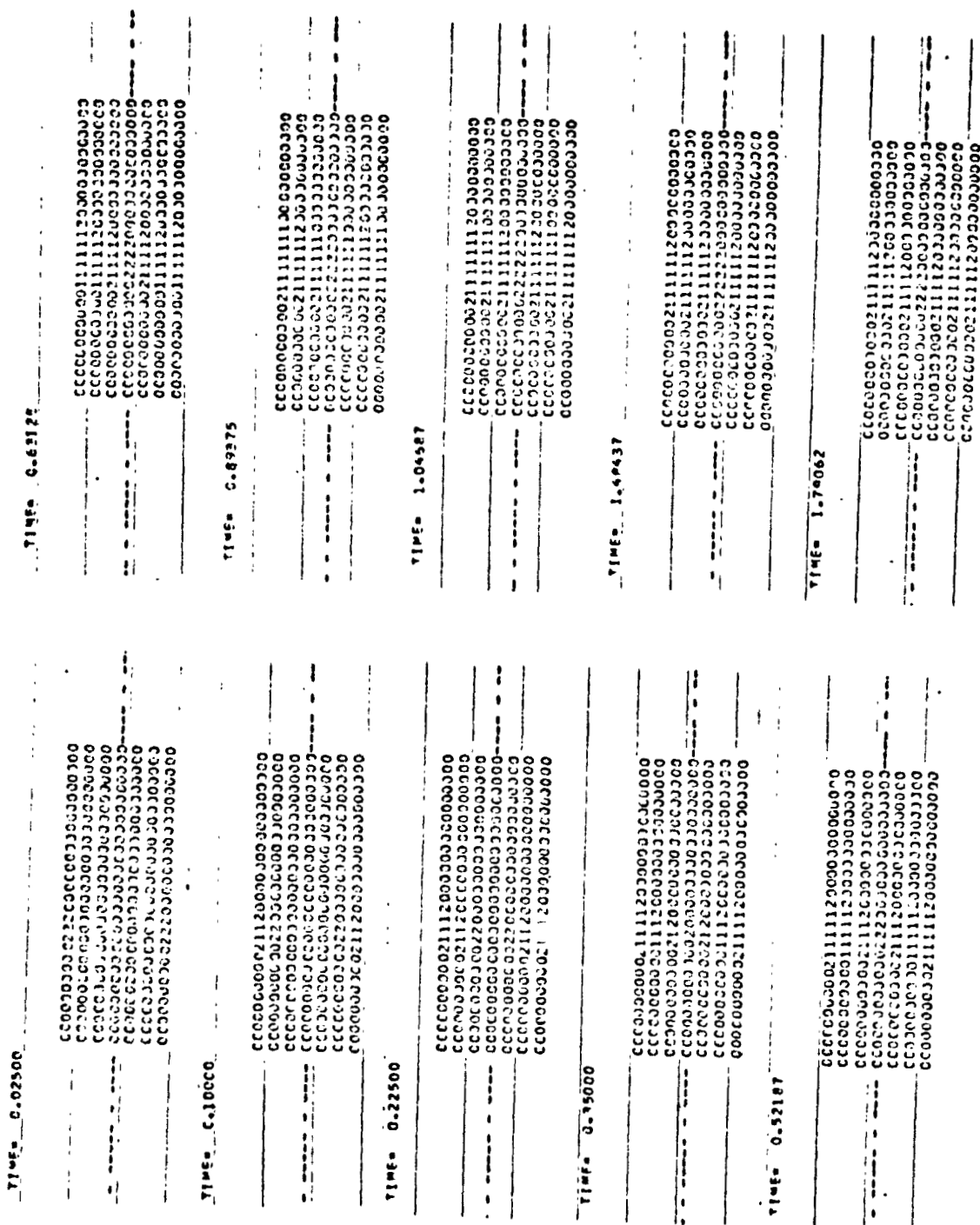
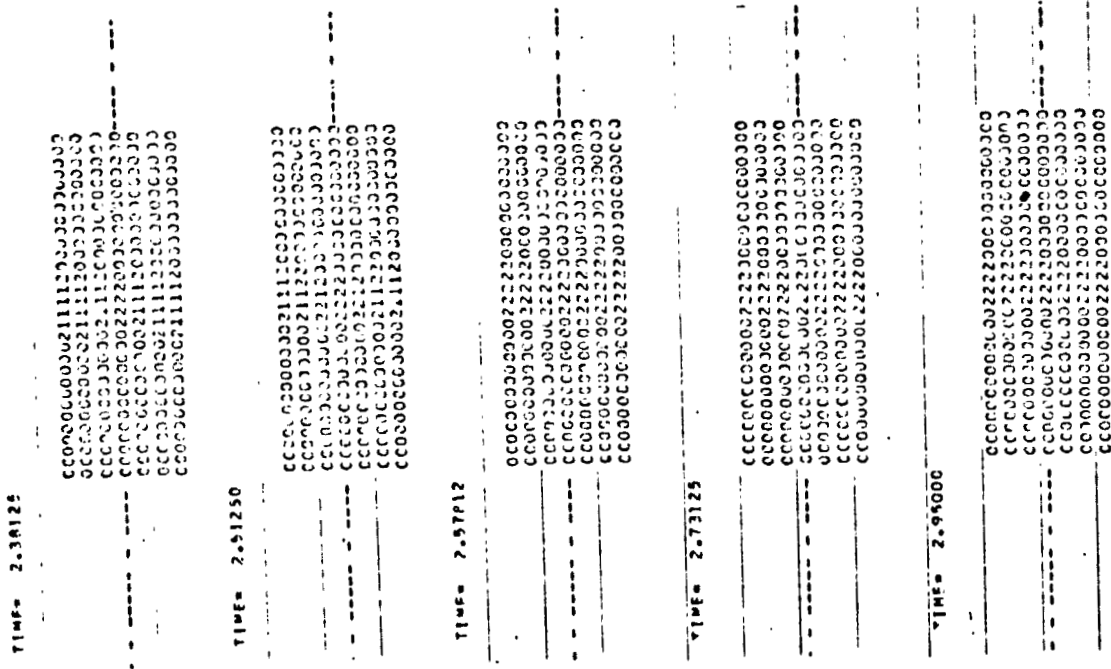


FIGURE: 14 . Run 44 - MELT ZONES



ORIGINAL PAGE IS  
OF POOR QUALITY

Figure 14. Run 44 (Continued)

The figure displays a 4x4 grid of 16 binary matrices, each representing a state transition at a specific time step. The matrices are arranged in a 4x4 grid, with labels indicating the time step for each matrix.

- TIME = 0.02500**: Matrix 1 (top-left). Contains mostly zeros with scattered ones, notably at positions (1,1), (2,2), (3,3), (4,4), (5,5), (6,6), (7,7), (8,8), (9,9), (10,10), (11,11), and (12,12).
- TIME = 0.12500**: Matrix 2 (top-middle). Contains mostly zeros with ones at positions (1,1), (2,2), (3,3), (4,4), (5,5), (6,6), (7,7), (8,8), (9,9), (10,10), (11,11), and (12,12).
- TIME = 0.25000**: Matrix 3 (top-right). Contains mostly zeros with ones at positions (1,1), (2,2), (3,3), (4,4), (5,5), (6,6), (7,7), (8,8), (9,9), (10,10), (11,11), and (12,12).
- TIME = 0.37500**: Matrix 4 (bottom-left). Contains mostly zeros with ones at positions (1,1), (2,2), (3,3), (4,4), (5,5), (6,6), (7,7), (8,8), (9,9), (10,10), (11,11), and (12,12).
- TIME = 0.50000**: Matrix 5 (bottom-middle). Contains mostly zeros with ones at positions (1,1), (2,2), (3,3), (4,4), (5,5), (6,6), (7,7), (8,8), (9,9), (10,10), (11,11), and (12,12).
- TIME = 0.62500**: Matrix 6 (bottom-right). Contains mostly zeros with ones at positions (1,1), (2,2), (3,3), (4,4), (5,5), (6,6), (7,7), (8,8), (9,9), (10,10), (11,11), and (12,12).
- TIME = 1.04687**: Matrix 7 (top-left). Contains mostly zeros with ones at positions (1,1), (2,2), (3,3), (4,4), (5,5), (6,6), (7,7), (8,8), (9,9), (10,10), (11,11), and (12,12).
- TIME = 1.20000**: Matrix 8 (top-middle). Contains mostly zeros with ones at positions (1,1), (2,2), (3,3), (4,4), (5,5), (6,6), (7,7), (8,8), (9,9), (10,10), (11,11), and (12,12).
- TIME = 1.37500**: Matrix 9 (top-right). Contains mostly zeros with ones at positions (1,1), (2,2), (3,3), (4,4), (5,5), (6,6), (7,7), (8,8), (9,9), (10,10), (11,11), and (12,12).
- TIME = 1.65937**: Matrix 10 (bottom-left). Contains mostly zeros with ones at positions (1,1), (2,2), (3,3), (4,4), (5,5), (6,6), (7,7), (8,8), (9,9), (10,10), (11,11), and (12,12).
- TIME = 1.94375**: Matrix 11 (bottom-middle). Contains mostly zeros with ones at positions (1,1), (2,2), (3,3), (4,4), (5,5), (6,6), (7,7), (8,8), (9,9), (10,10), (11,11), and (12,12).
- TIME = 2.22812**: Matrix 12 (bottom-right). Contains mostly zeros with ones at positions (1,1), (2,2), (3,3), (4,4), (5,5), (6,6), (7,7), (8,8), (9,9), (10,10), (11,11), and (12,12).

**Figure 1.5.** Run 49 = MELT ZONES

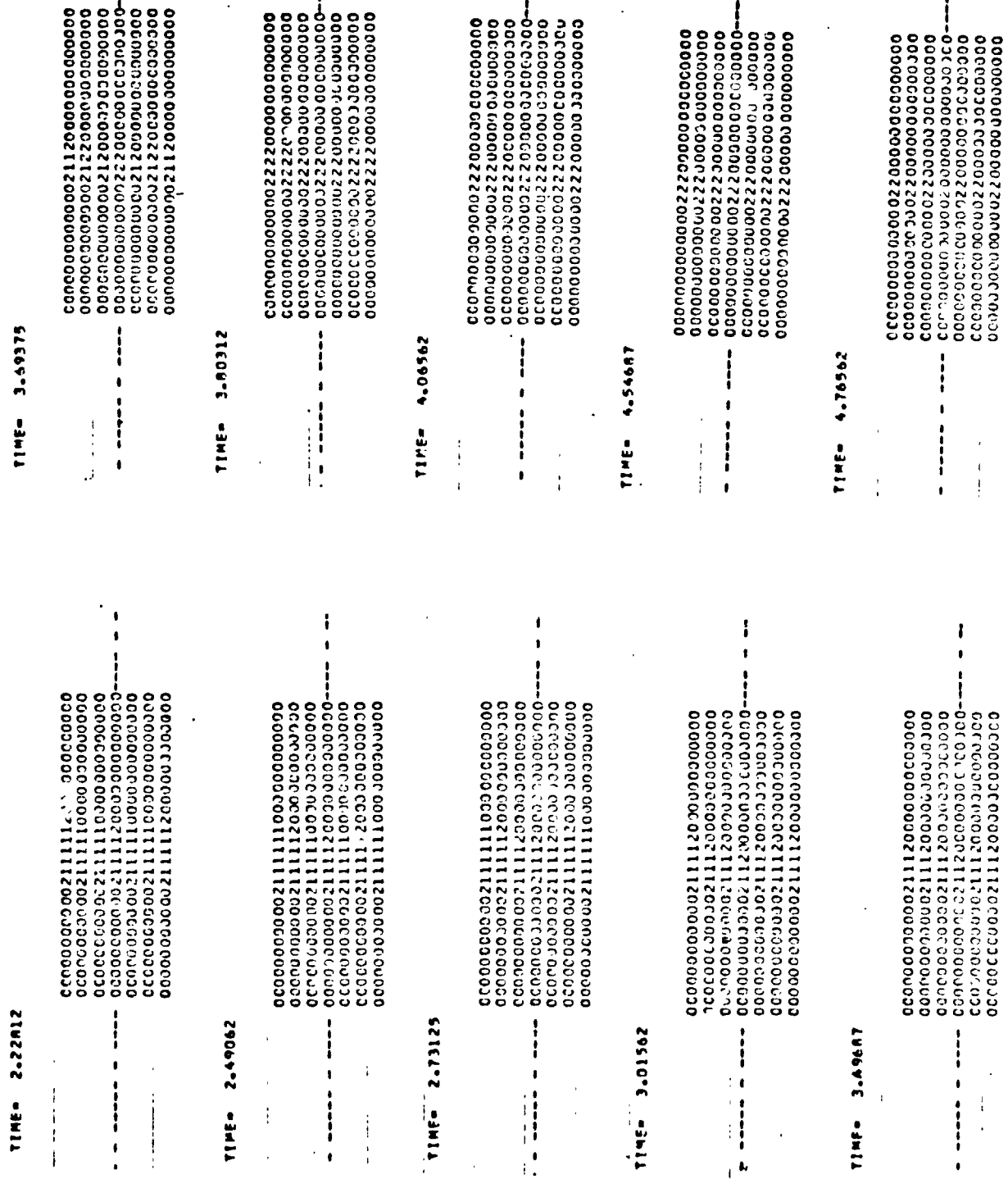


Figure 15. Run 49 (Continued)

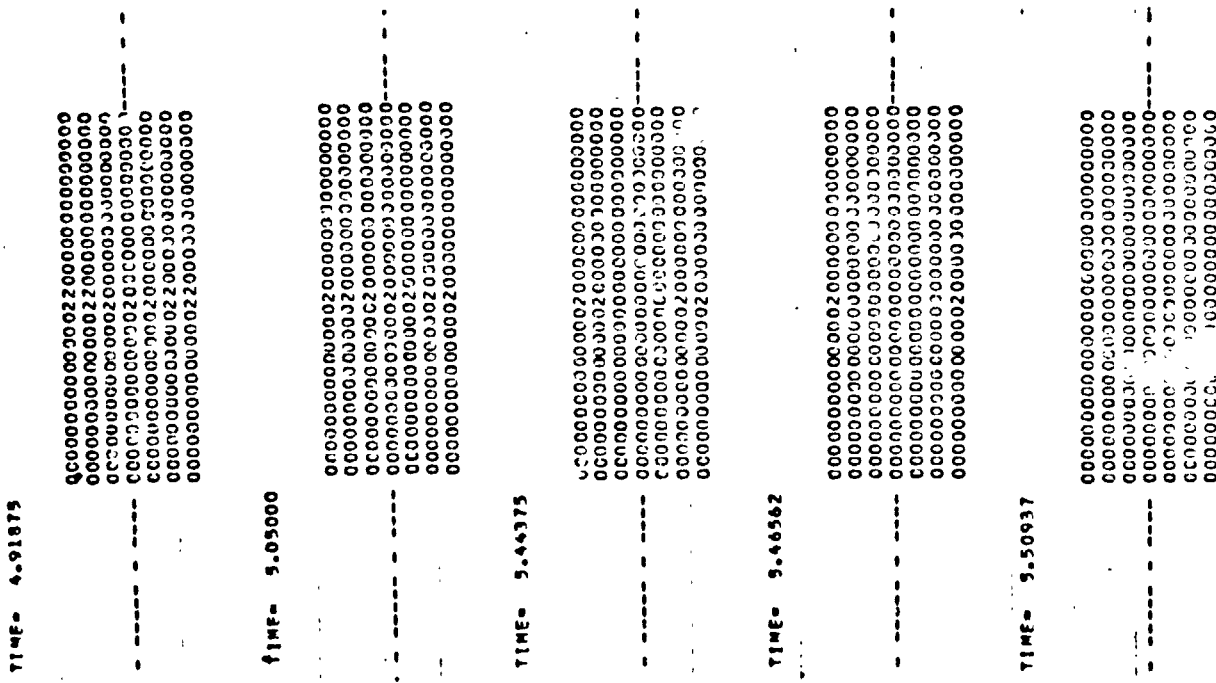


Figure 15. Run 4c (Continued).

TIME= 0.02500

0C0000000002222220000000000  
C0000001000000000000000000  
0000000000000000000000000  
- - - - - 0000000000000000000000000  
0000000000000000000000000  
0000000000000000000000000  
0000000000000000000000000

TIME= 0.37500

CC00000000022222000000000  
C00000000000000000000000  
00000000000000000000000  
- - - - - 00000000000000000000000  
00000000000000000000000  
00000000000000000000000  
00000000000000000000000

TIME= 0.71875

000000000000022220000000000  
0000000000000000000000000  
0000000000000000000000000  
- - - - - 00000000000000000000000  
00000000000000000000000  
00000000000000000000000  
00000000000000000000000

TIME= 1.09062

000000000000022220000000000  
0001000000000000000000000  
C00000000000000000000000  
- - - - - 00000000000000000000000  
00000000000000000000000  
00000000000000000000000  
00000000000000000000000

TIME= 1.87812

CC00000000000000000000000  
0000000000000000000000000  
0000000000000000000000000  
- - - - - 00000000000000000000000  
00000000000000000000000  
00000000000000000000000  
00000000000000000000000

ORIGINAL PAGE IS  
OF POOR QUALITY

Figure 16. Run 55 - MELT ZONES

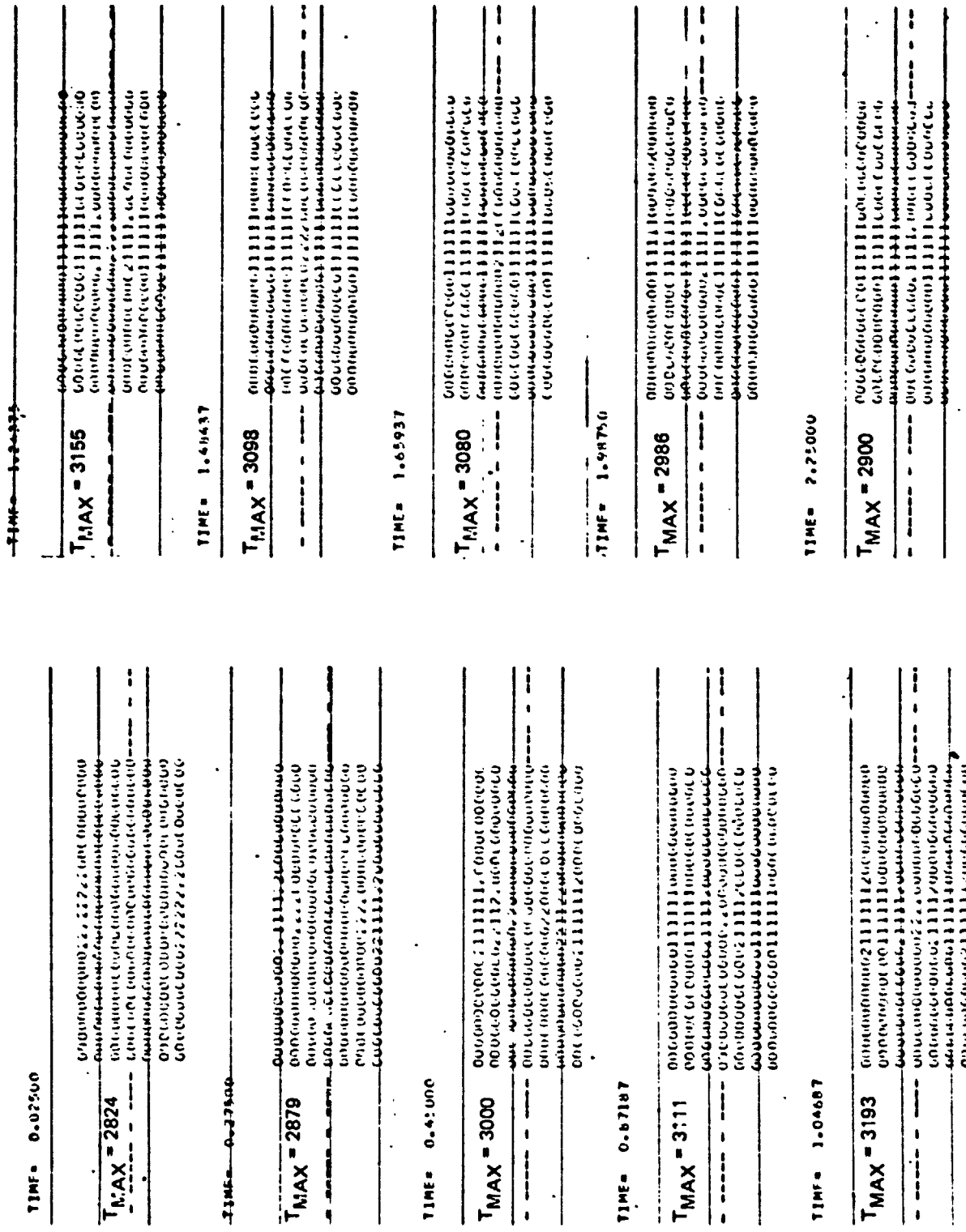


*Figure 17. Run 56. - MELT ZONES*

TIME = 7.00.00.00 7

ORIGINAL PAGE IS  
OF POOR QUALITY

卷之三

Acute myocardial infarction  
non-ST-elevation myocardial infarction  
ST-elevation myocardial infarction  
Other acute coronary syndrome  
Percutaneous intervention  
Cardiac catheterization

TINT 2 2004 34

T<sub>MAX</sub> = 2626

0-711878 3223437

卷之三

**TMAX = 2573** *one tenth of one percent connected  
to G-1, G-2, G-3, G-4 and G-5, and one percent to G-6-G-10  
and one percent to G-11, G-12 and G-13 connected. One  
percent connects to G-14, G-15, G-16, G-17, G-18, G-19, G-20,  
G-21, G-22, G-23, G-24, G-25, G-26, G-27, G-28, G-29, G-30, G-31,  
G-32, G-33, G-34, G-35, G-36, G-37, G-38, G-39, G-40, G-41, G-42,  
G-43, G-44, G-45, G-46, G-47, G-48, G-49, G-50, G-51, G-52, G-53,  
G-54, G-55, G-56, G-57, G-58, G-59, G-60, G-61, G-62, G-63, G-64,  
G-65, G-66, G-67, G-68, G-69, G-70, G-71, G-72, G-73, G-74, G-75,  
G-76, G-77, G-78, G-79, G-80, G-81, G-82, G-83, G-84, G-85, G-86,  
G-87, G-88, G-89, G-90, G-91, G-92, G-93, G-94, G-95, G-96, G-97,  
G-98, G-99, G-100, G-101, G-102, G-103, G-104, G-105, G-106, G-107,  
G-108, G-109, G-110, G-111, G-112, G-113, G-114, G-115, G-116,  
G-117, G-118, G-119, G-120, G-121, G-122, G-123, G-124, G-125,  
G-126, G-127, G-128, G-129, G-130, G-131, G-132, G-133, G-134,  
G-135, G-136, G-137, G-138, G-139, G-140, G-141, G-142, G-143,  
G-144, G-145, G-146, G-147, G-148, G-149, G-150, G-151, G-152,  
G-153, G-154, G-155, G-156, G-157, G-158, G-159, G-160, G-161,  
G-162, G-163, G-164, G-165, G-166, G-167, G-168, G-169, G-170,  
G-171, G-172, G-173, G-174, G-175, G-176, G-177, G-178, G-179,  
G-180, G-181, G-182, G-183, G-184, G-185, G-186, G-187, G-188,  
G-189, G-190, G-191, G-192, G-193, G-194, G-195, G-196, G-197,  
G-198, G-199, G-200, G-201, G-202, G-203, G-204, G-205, G-206,  
G-207, G-208, G-209, G-210, G-211, G-212, G-213, G-214, G-215,  
G-216, G-217, G-218, G-219, G-220, G-221, G-222, G-223, G-224,  
G-225, G-226, G-227, G-228, G-229, G-230, G-231, G-232, G-233,  
G-234, G-235, G-236, G-237, G-238, G-239, G-240, G-241, G-242,  
G-243, G-244, G-245, G-246, G-247, G-248, G-249, G-250, G-251,  
G-252, G-253, G-254, G-255, G-256, G-257, G-258, G-259, G-259,*

**TMAX = 2573** OCT 1970 21:00Z  
DRAFT ON 19 JULY 1970 - SIGHTED  
THIS DAY, AND IS THEREFORE  
CONSISTENT WITH THE DATE  
OF THE OBSERVATION.  
CLOUDS ARE OVERCAST.  
THE CLOUDS ARE  
ABOUT 1000 FT THICK.  
THE CLOUDS ARE  
ABOUT 1000 FT THICK.

-7-  
1945. 4. 5. 27

On the 1st of October 1945, I went to the  
Ministry of Education to inquire about the  
possibility of getting a teaching position in  
the Ministry. I was told that there were no  
positions available at present.

Figure 17 Run 55 (Continued)

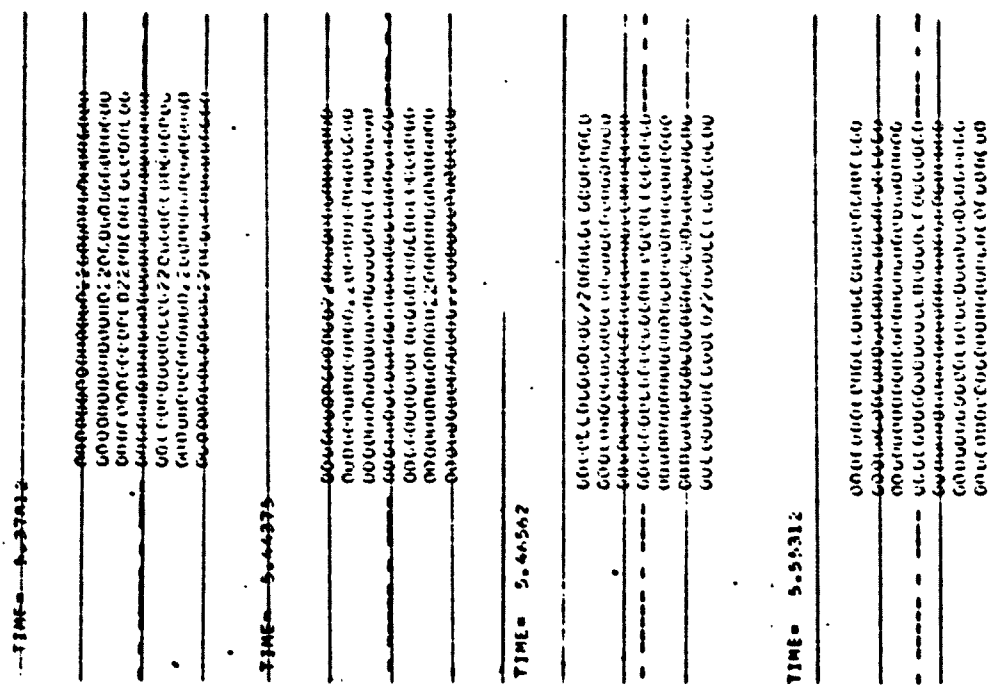


**Figure 17. Run 56 (Continued)**

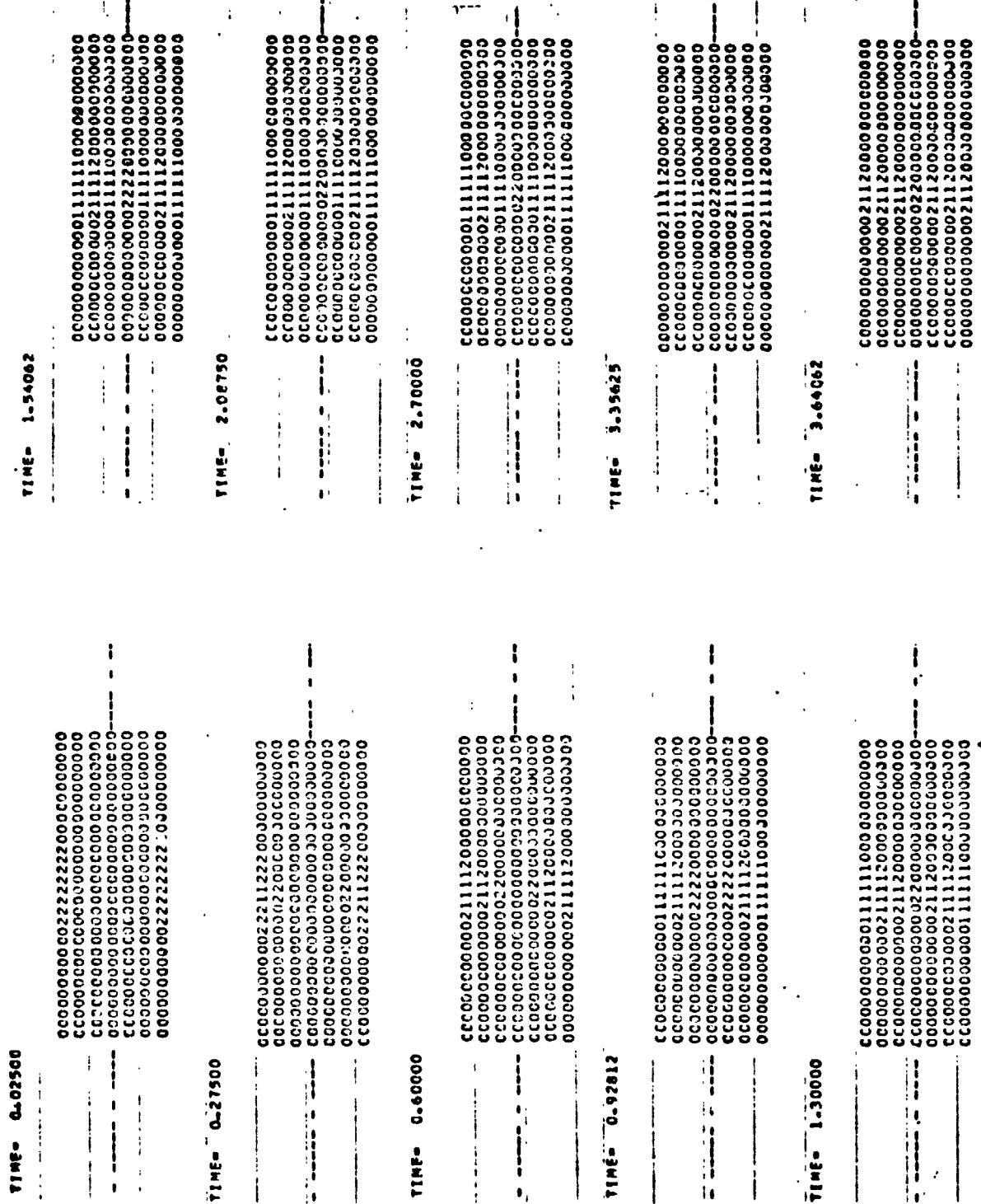


Figure 18. Run 60 - MELT ZONES

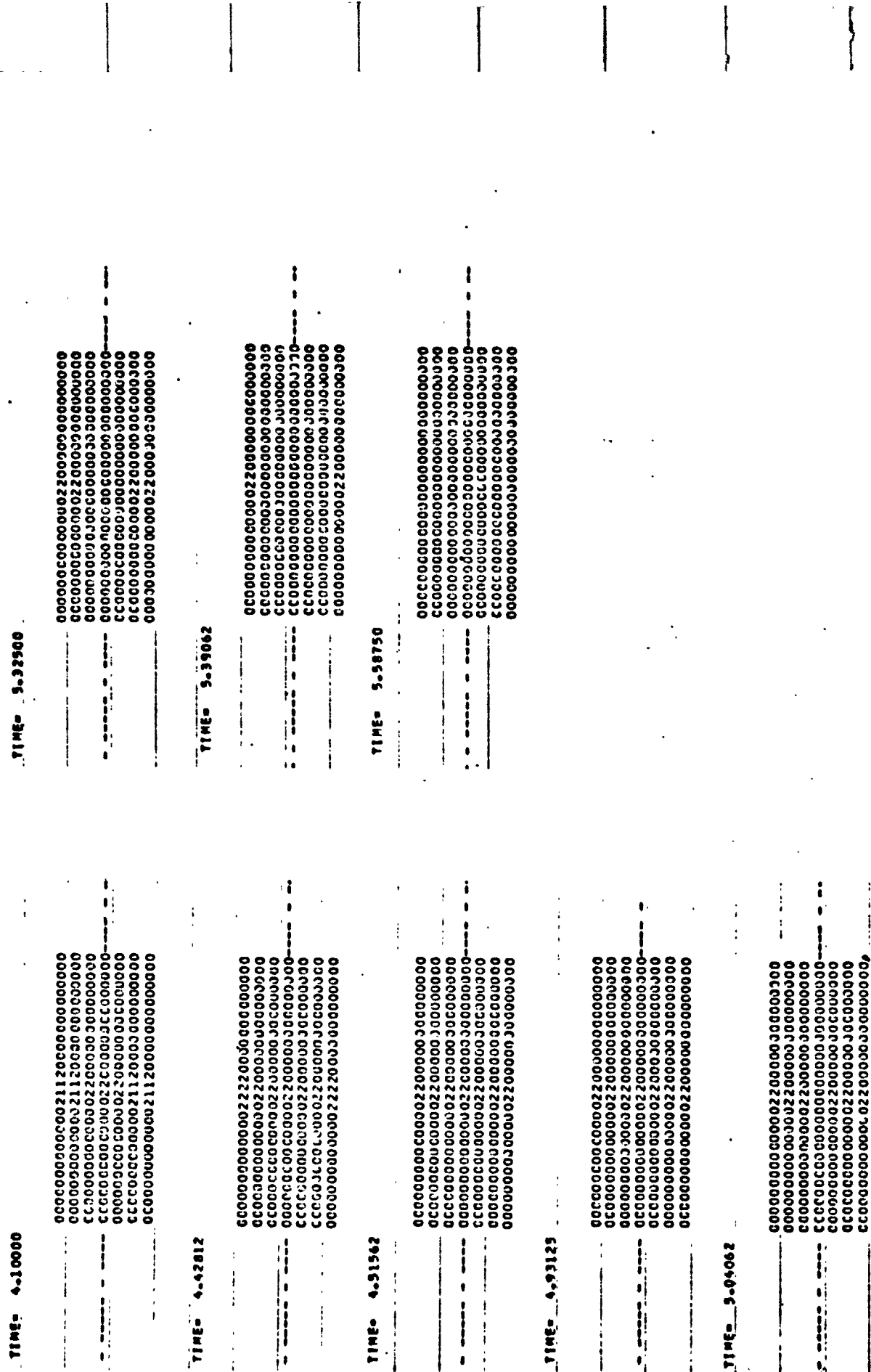
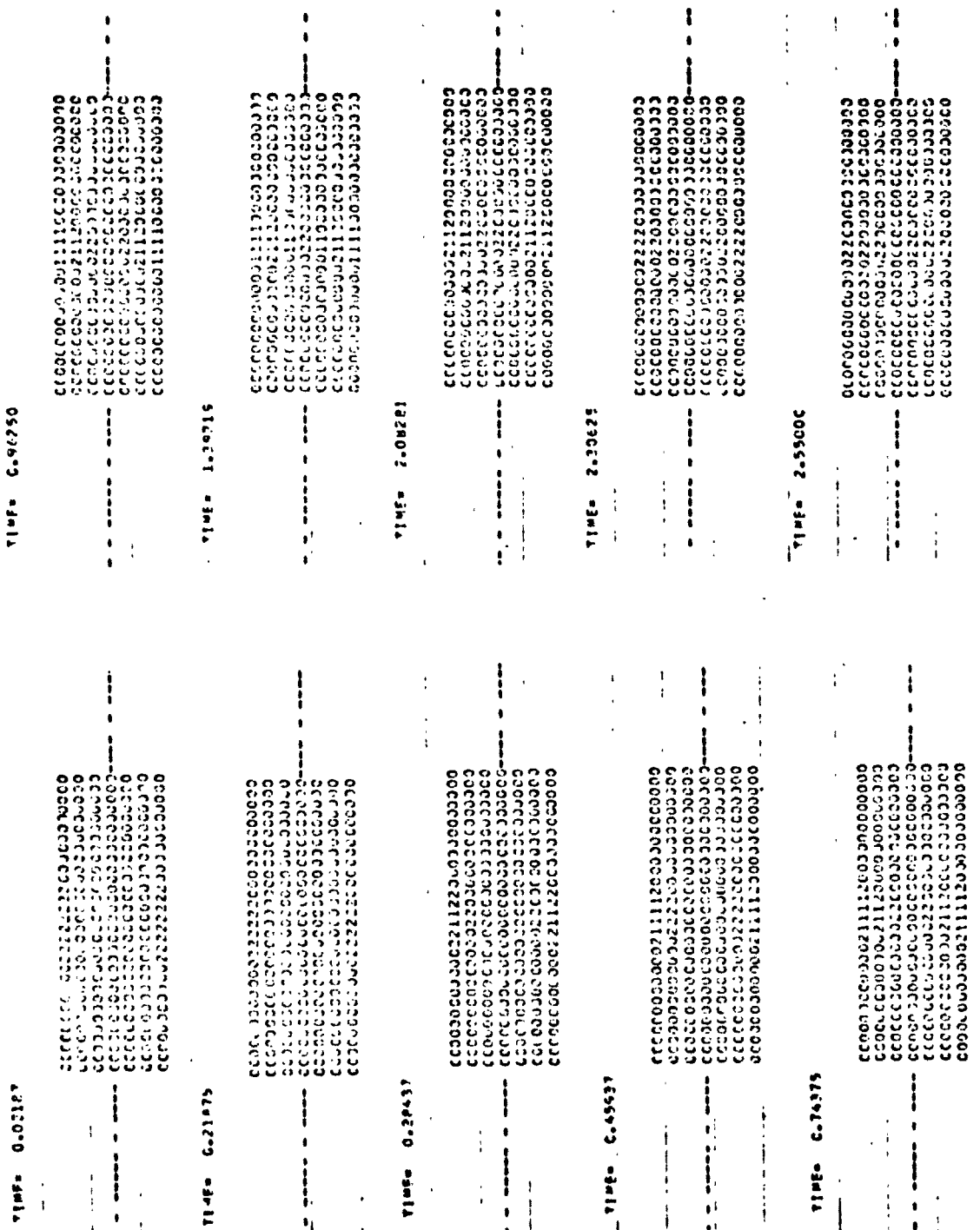


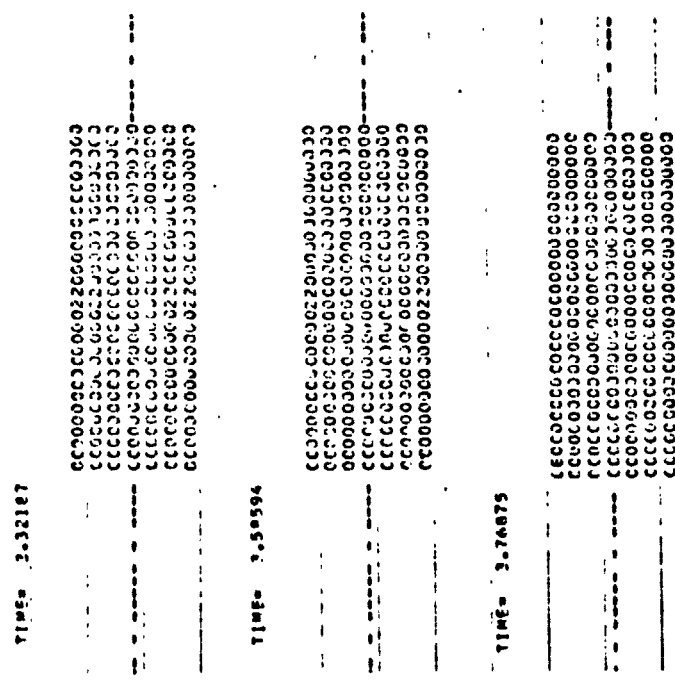
Figure 18. Run 60 (Continued)

**Figure 19. Run 62. - MELT ZONES**



ORIGINAL PAGE IS  
OF POOR QUALITY

*Figure 19. Run 62 (Continued)*



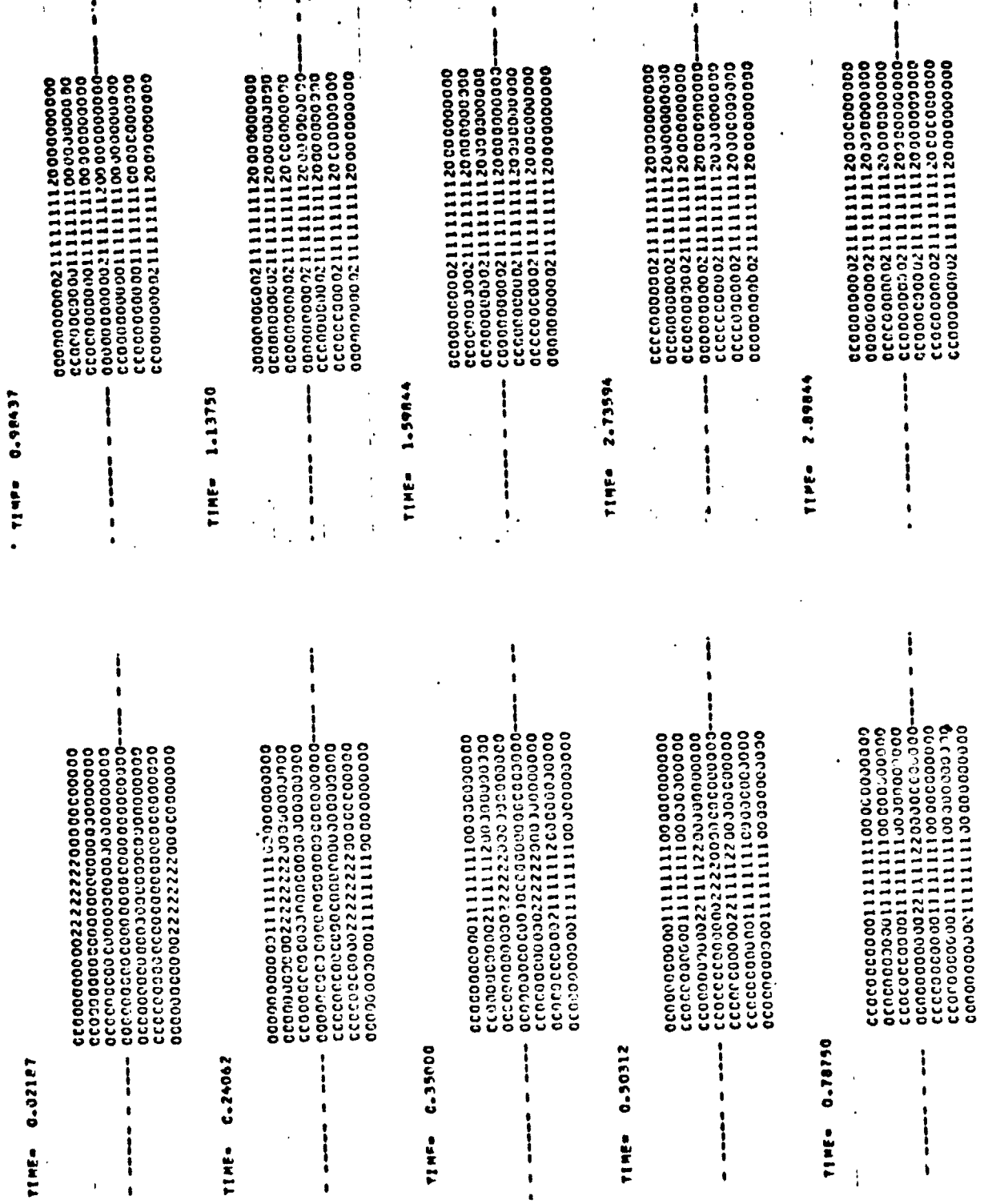
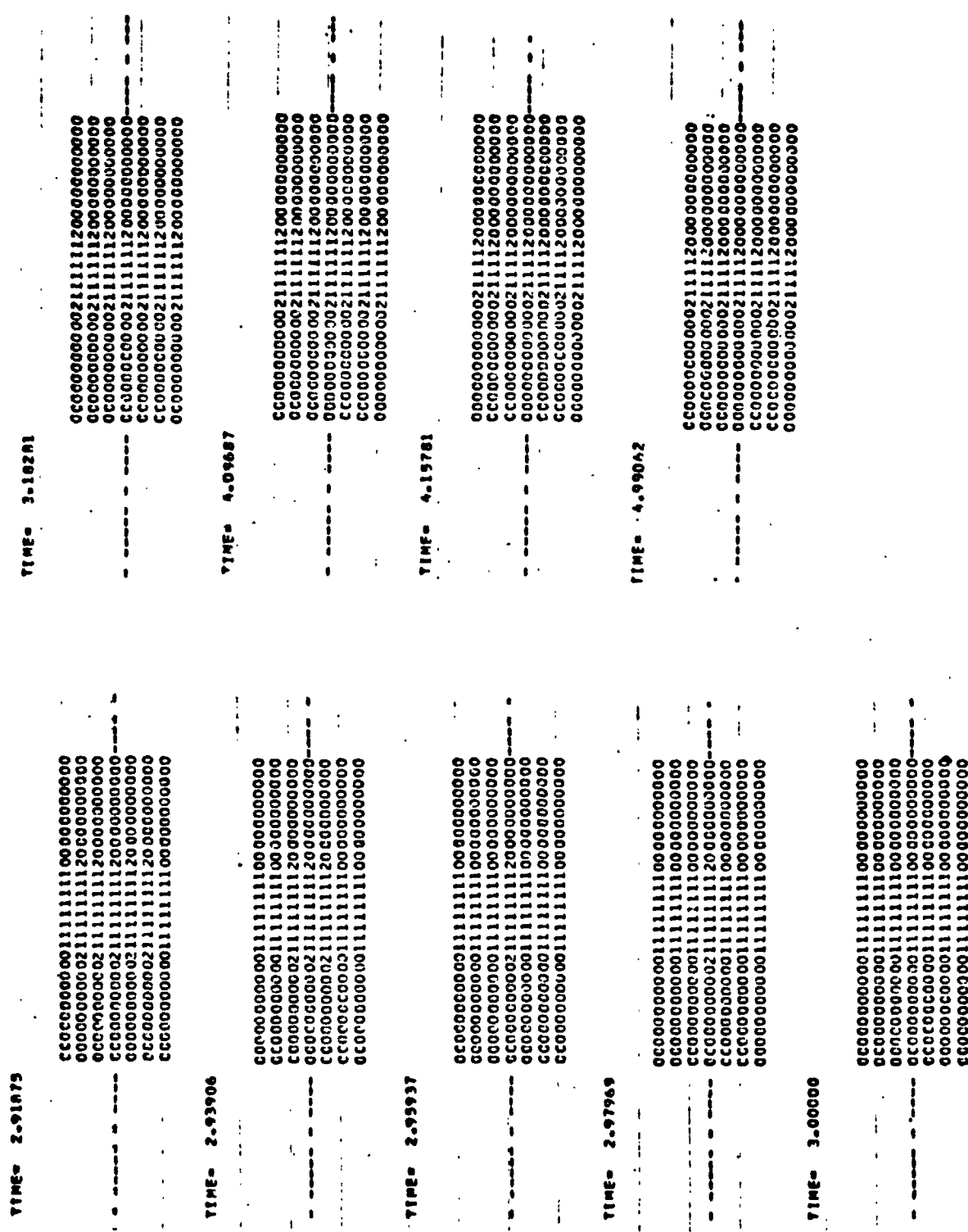


Figure 20. Run 65 – MELT ZONES



*Figure 20. Run 65 (Continued)*

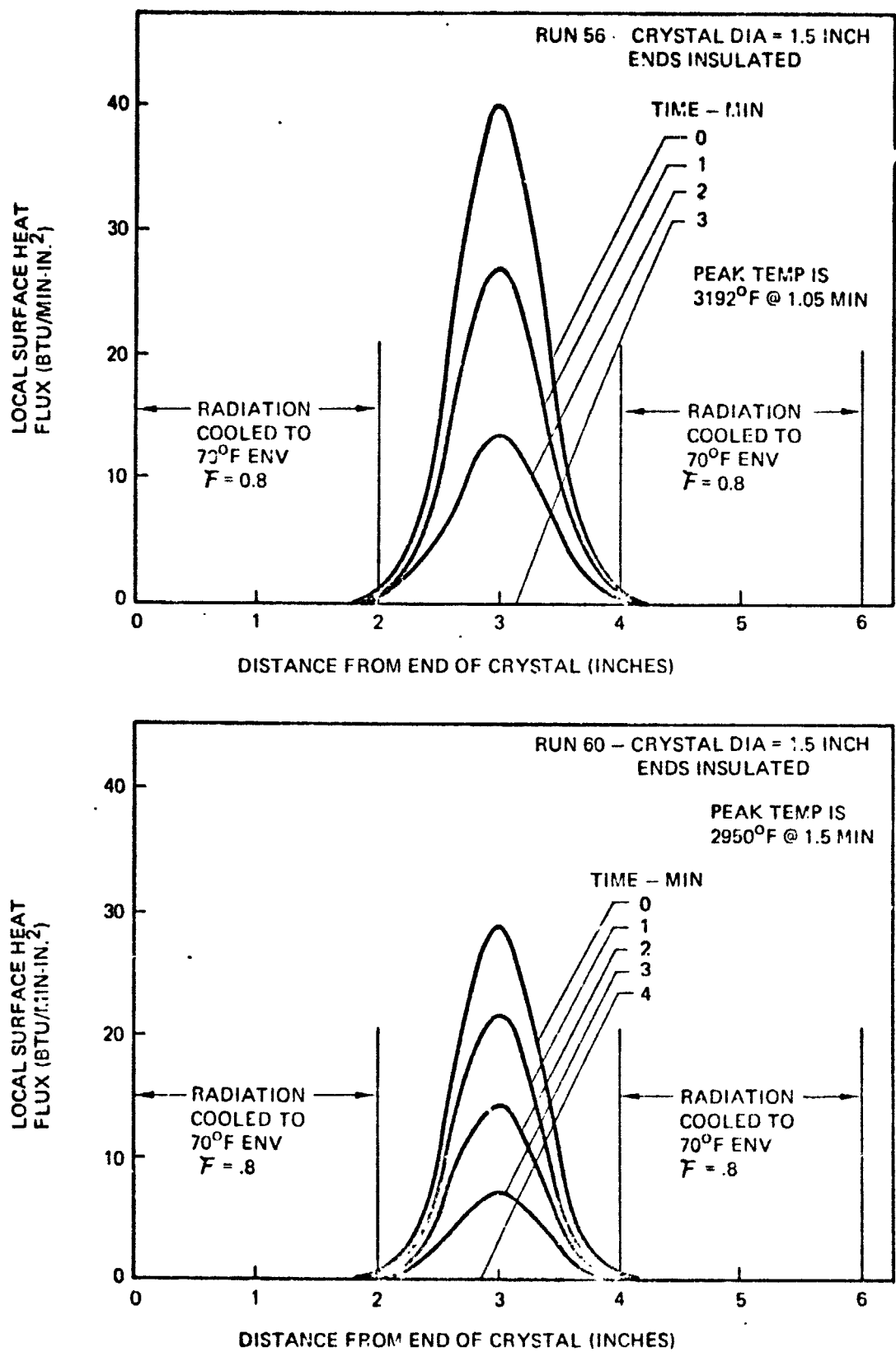
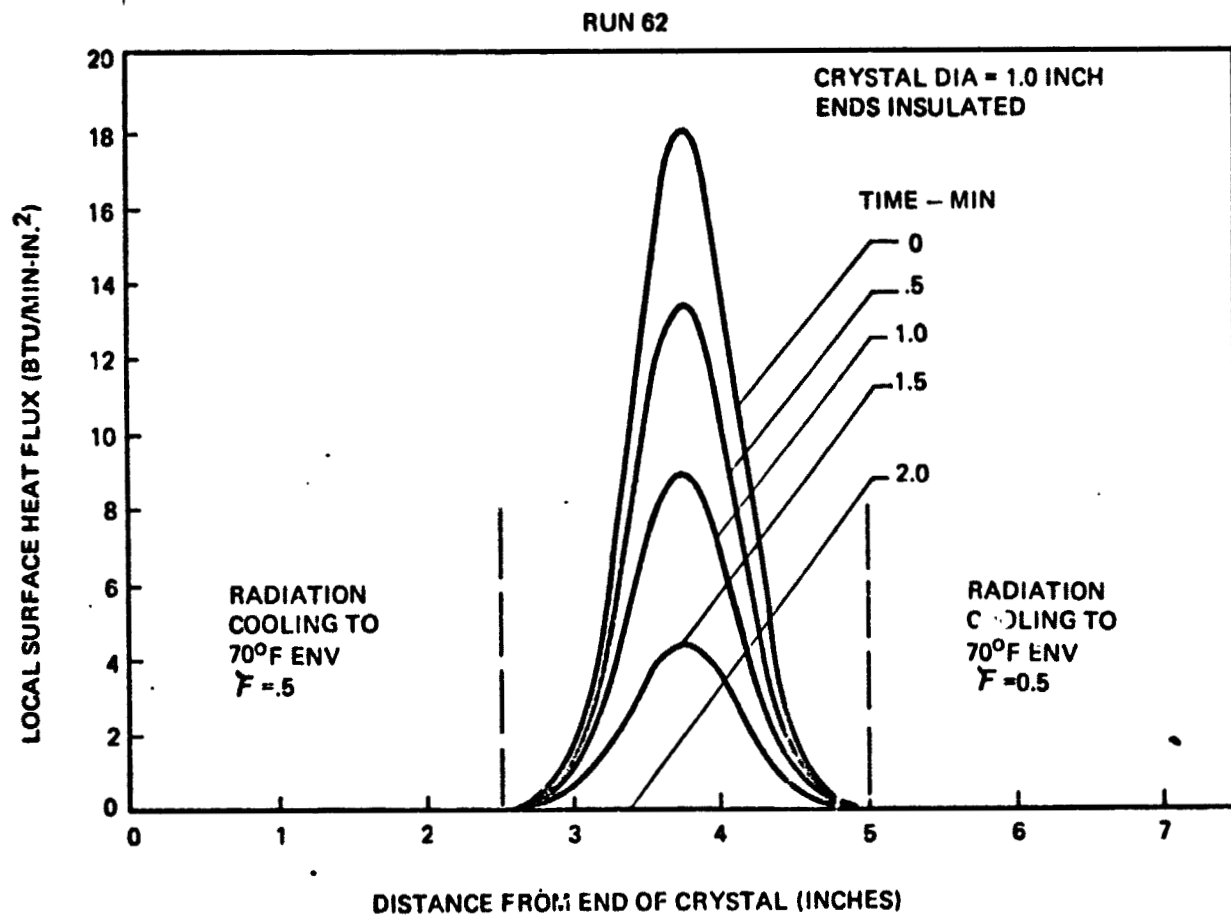
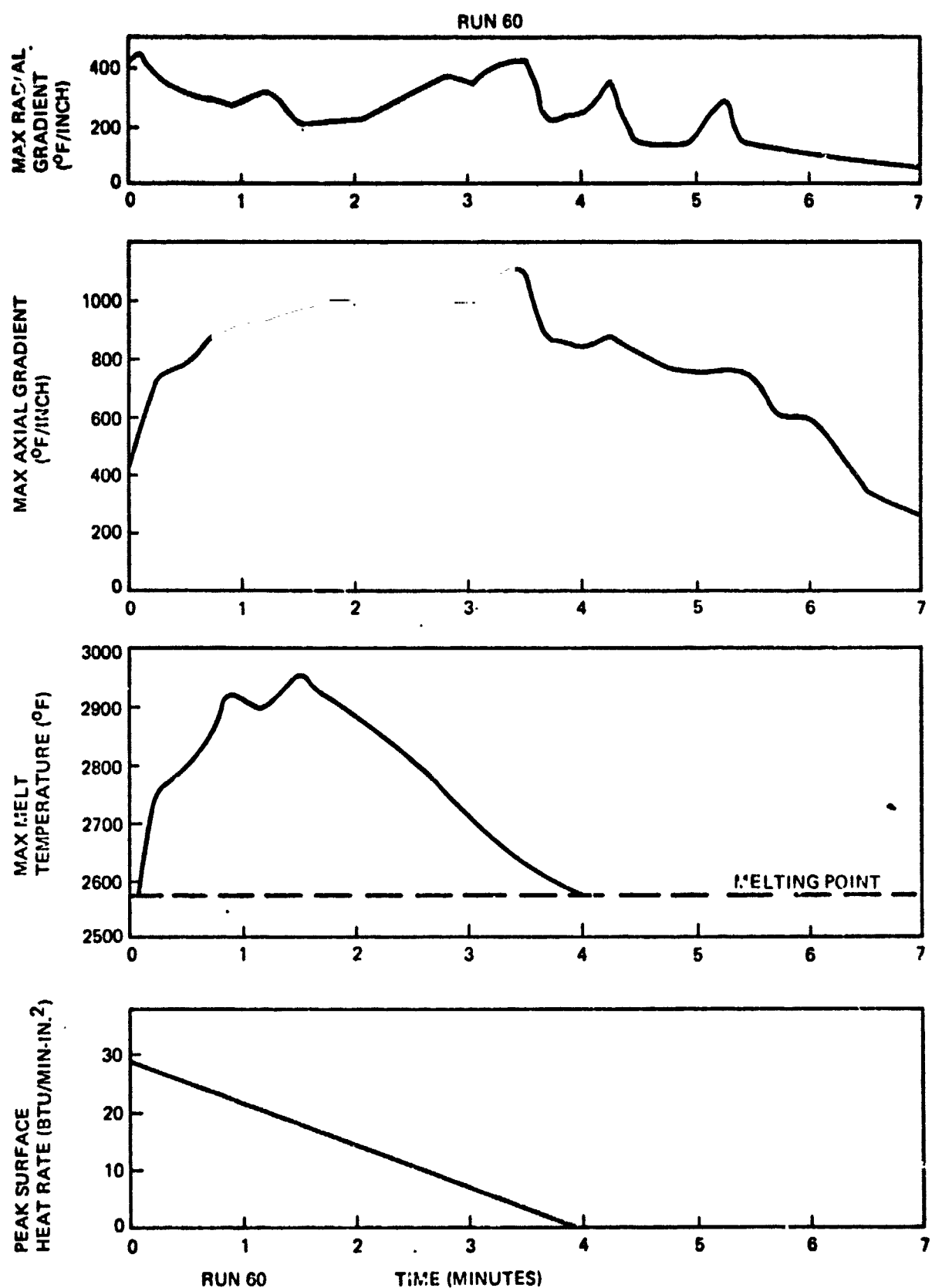


Figure 21  
SURFACE HEAT FLUX RUN 56 & 60



*Figure 22*  
SURFACE HEAT FLUX RUN E2



**Figure 23**  
**RUN 60 - TEMPERATURE GRADIENT & HEAT FLUX PROFILES**

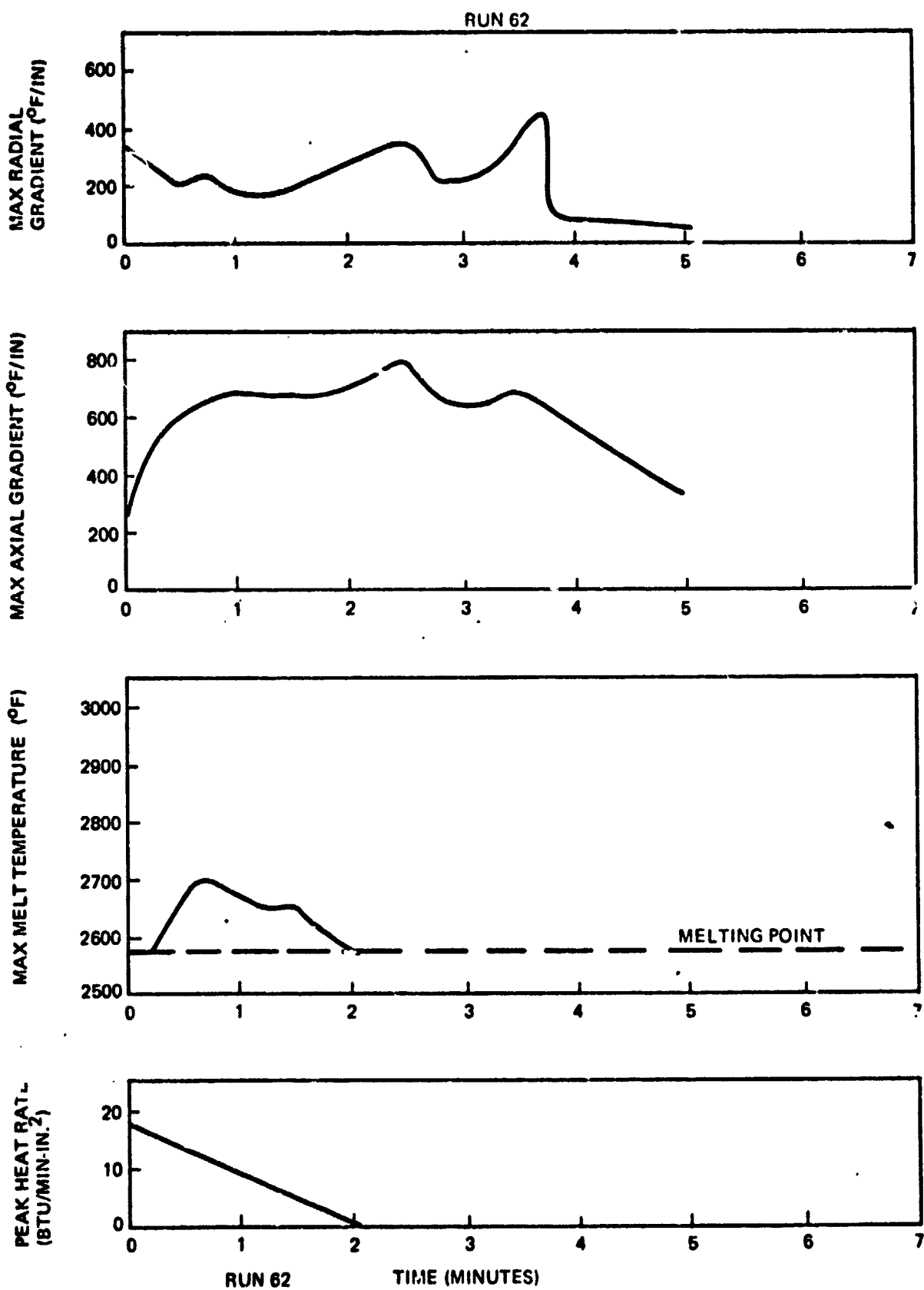


*Figure 24*  
RUN 62 - TEMPERATURE GRADIENT & HEAT FLUX PROFILES

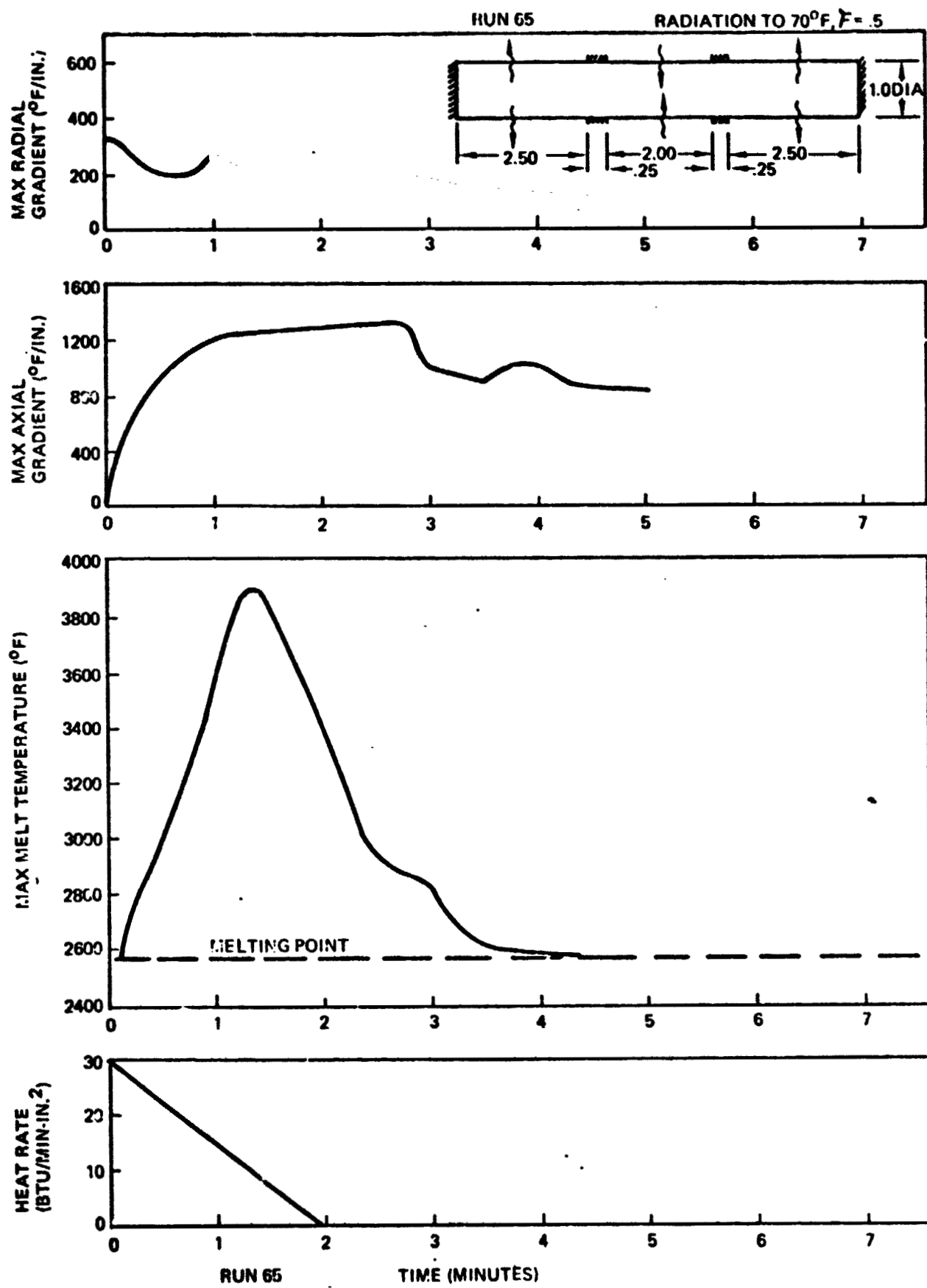
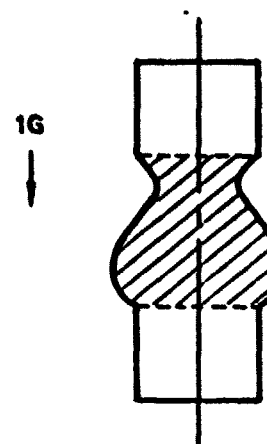
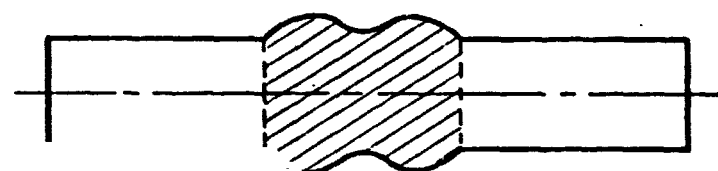


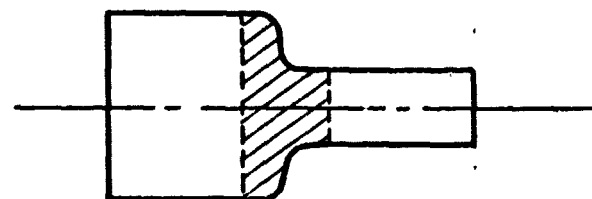
Figure 25  
RUN 65 - TEMPERATURE GRADIENT & HEAT FLUX PROFILES



(a) VERTICAL CYLINDER WITH GRAVITY



(b) FLOAT ZONE IN ZERO-G WITH ROTATION



(c) FLOAT ZONE BETWEEN DIFFERENT DIAMETERS

FIGURE: 26 . *Typical Body-of-Revolution Configurations*

MAP SHOWING NODE LOCATIONS AND BOUNDARY CONDITIONS

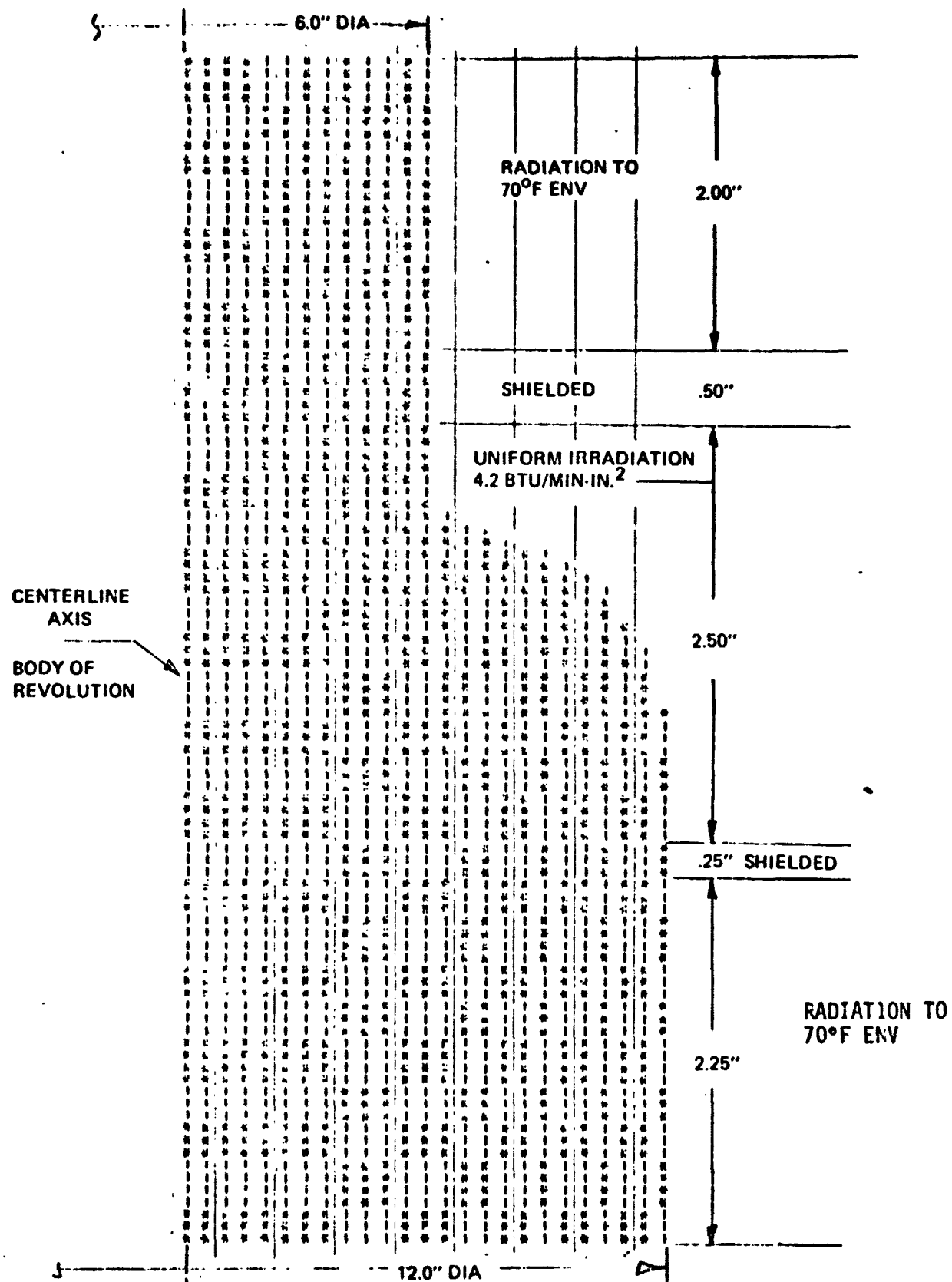


FIGURE : 27 Run 80 BODY OF REVOLUTION NODE MAP

INITIAL CONDITIONS - TIME = 0  
HEATING RATE = 551 BTU/MIN  
COOLING RATE = 772 BTU/MIN

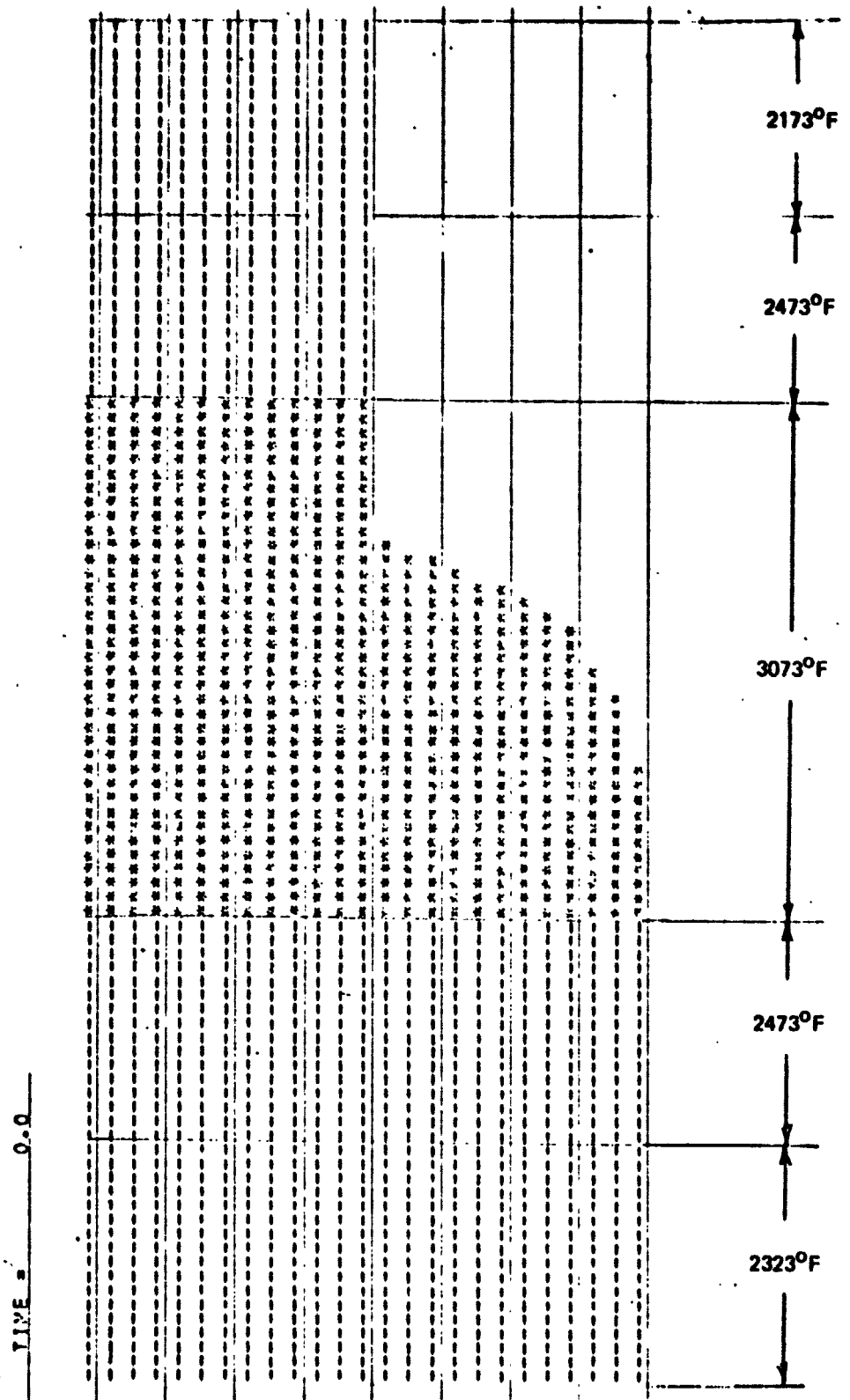


FIGURE: 28. Run 80 - MELT ZONE - TIME = 0

CONDITION AT TIME = 2.852 MIN  
HEATING RATE = 551 BTU/MIN  
COOLING RATE = 594 BTU/MIN

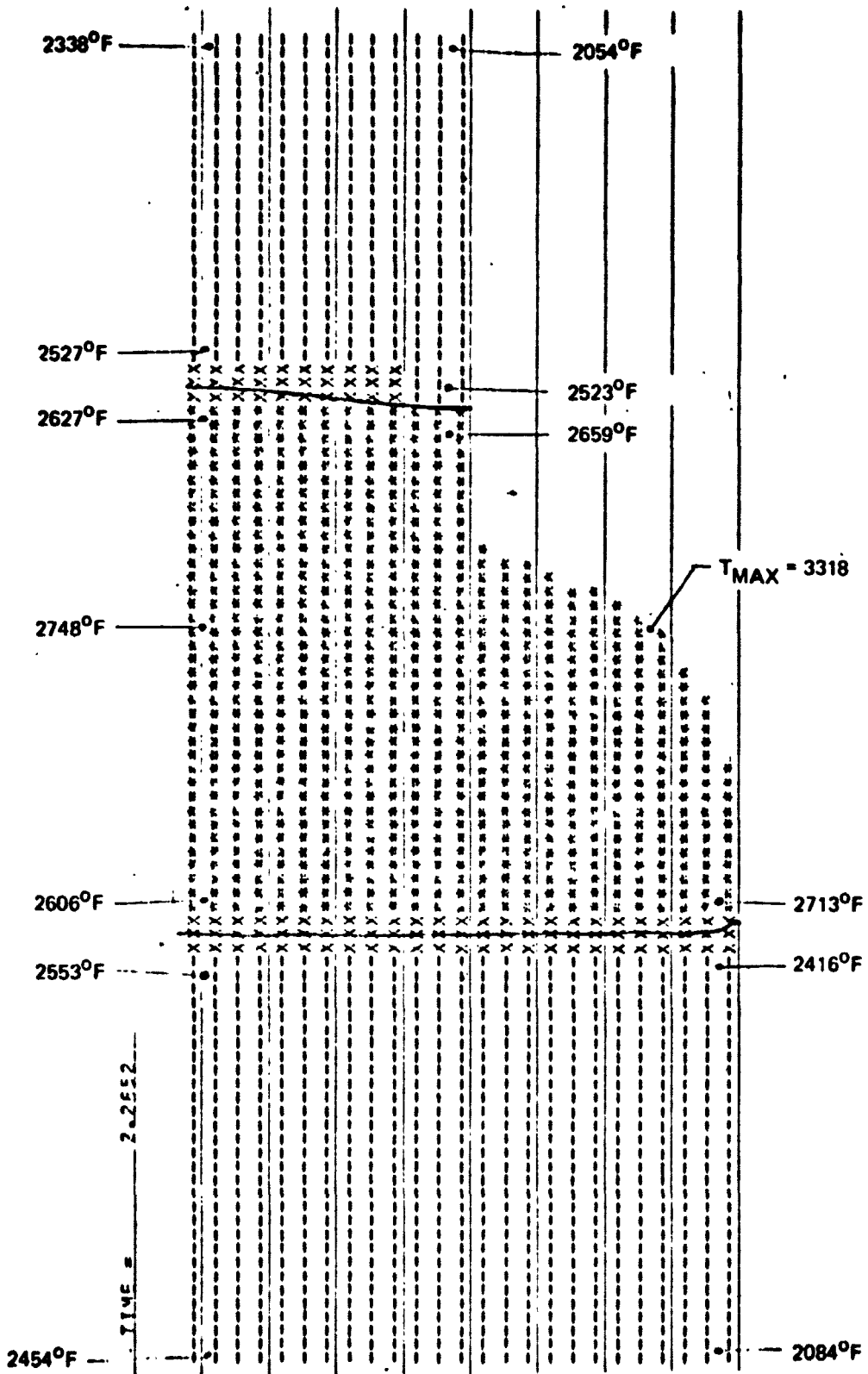


FIGURE: 29. Run 80 - MELT ZONE - TIME = 2.852 MIN.

MELT ZONE NODE MAP

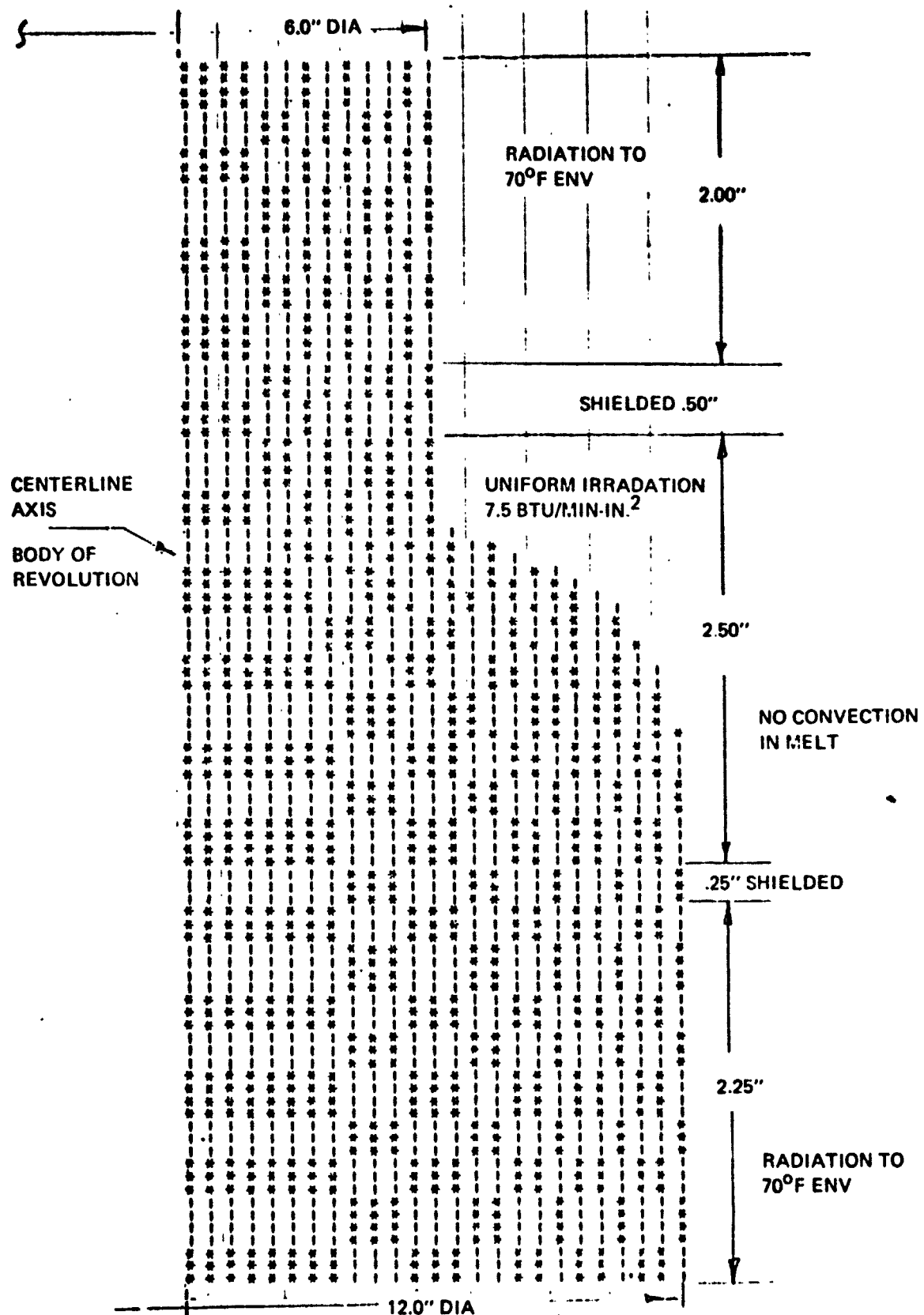
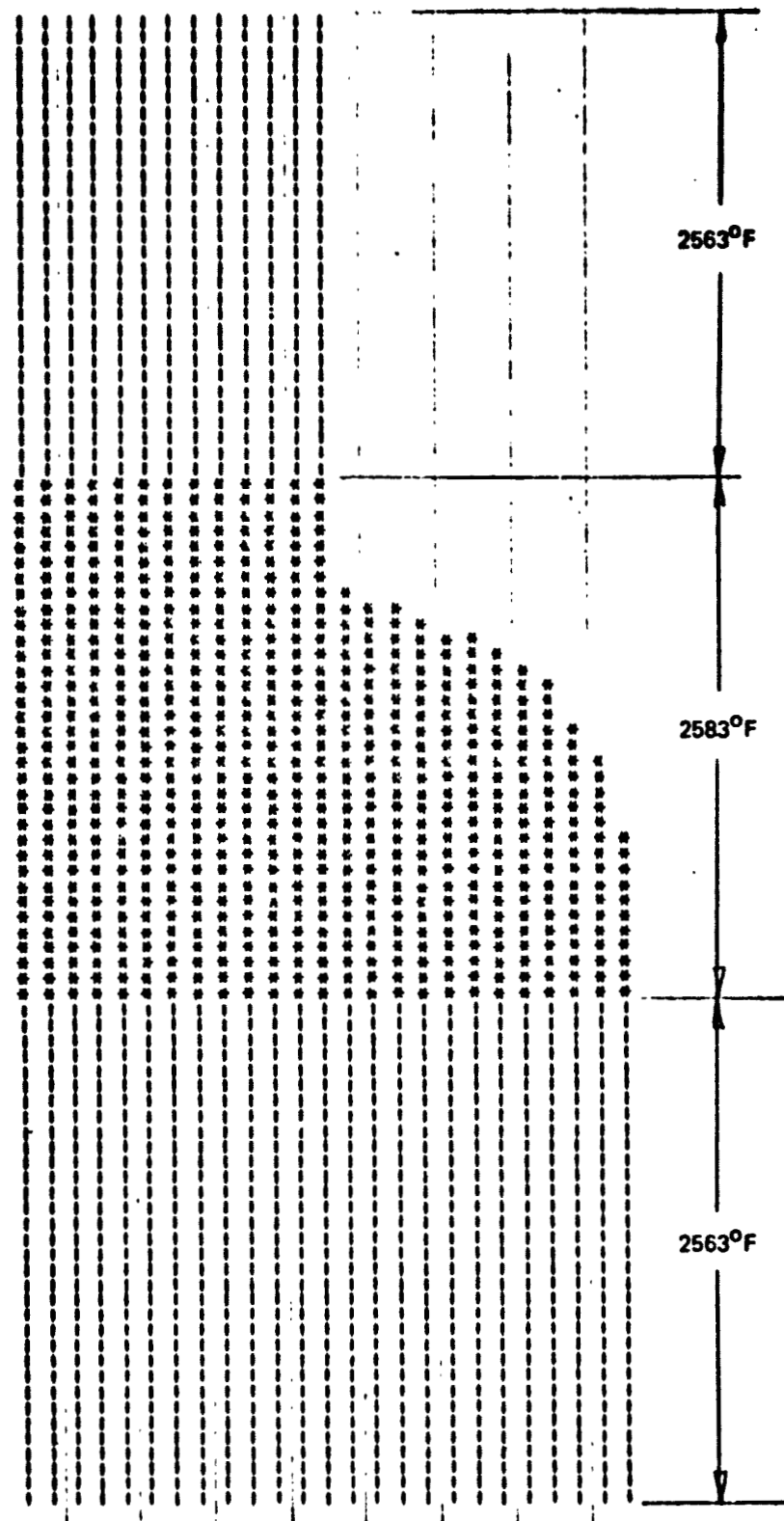


Figure 30. Run 72 - MELT ZONE NODE MAP

**INITIAL CONDITIONS - TIME = 0**  
**HEATING RATE = 984 BTU/MIN**  
**COOLING RATE = 1013 BTU/MIN**



**Figure 31. MELT ZONE TIME = 0 RUN 72**

CONDITION AT TIME = 7.8 MIN

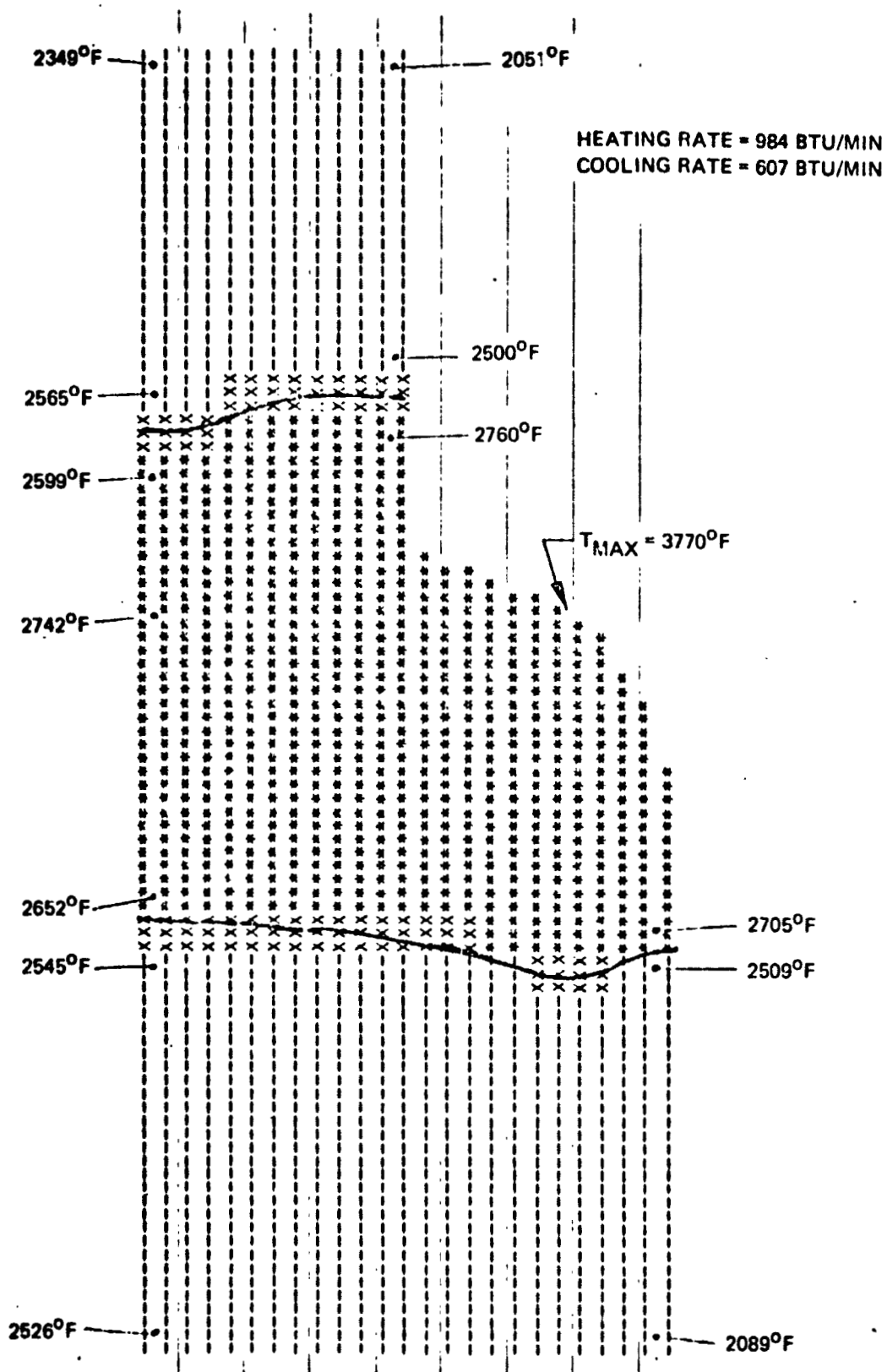


Figure 32. MELT ZONE TIME = 7.8 MIN. RUN 72